CANCER
COMMUNICATIONS
Open Access

ORIGINAL ARTICLE

SDCBP-AS1 destabilizes β-catenin by regulating ubiquitination and SUMOylation of hnRNP K to suppress gastric tumorigenicity and metastasis

Jing Han[1] | **Menglin Nie**[2] | **Cong Chen**[1] | **Xiaojing Cheng**[1] | **Ting Guo**[1] | **Longtao Huangfu**[1] | **Xiaomei Li**[1] | **Hong Du**[1] | **Xiaofang Xing**[1] | **Jiafu Ji**[1,3]

[1]Department of Gastrointestinal Cancer Translational Research Laboratory, Key Laboratory of Carcinogenesis and Translational Research (Ministry of Education), Peking University Cancer Hospital, Beijing Institute for Cancer Research, Beijing 100142, P. R. China

[2]Department of Radiation Oncology, Beijing Tiantan Hospital, Capital Medical University, Beijing 100070, P. R. China

[3]Department of Gastrointestinal Surgery, Key Laboratory of Carcinogenesis and Translational Research (Ministry of Education), Peking University Cancer Hospital, Beijing Institute for Cancer Research, Beijing 100142, P. R. China

Correspondence
Jiafu Ji or Xiaofang Xing, Department of Gastrointestinal Cancer Translational Research Laboratory, Key Laboratory of Carcinogenesis and Translational Research (Ministry of Education), Peking University Cancer Hospital, Beijing Institute for Cancer Research, #52 Fucheng Road, Beijing, 100142, P. R. China. FAX: 0086-010-88196760.
Email: jijiafu@hsc.pku.edu.cn, xingxiaofang@bjmu.edu.cn

Funding information
the National High Technology Research and Development Program of China,

Abstract

Background: Gastric cancer (GC) is among the most malignant tumors, yet the pathogenesis is not fully understood, especially the lack of detailed information about the mechanisms underlying long non-coding RNA (lncRNA)-mediated post-translational modifications. Here, the molecular mechanisms and clinical significance of the novel lncRNA syndecan-binding protein 2-antisense RNA 1 (SDCBP2-AS1) in the tumorigenesis and progression of GC were investigated.

Methods: The expression levels of SDCBP2-AS1 in 132 pairs of GC and adjacent normal tissues were compared, and the biological functions were assessed in vitro and in vivo. RNA pull-down and immunoprecipitation assays

Abbreviations: APC, adenomatous polyposis coli; β-TrCP, β-transducin repeat-containing protein; CHX, cycloheximide; CI, confidence interval; CTNNB1, catenin beta 1; DFS, disease-free survival; EPDR1, ependymin-related 1; FISH, fluorescence in situ hybridization; GAPDH, glyceraldehyde 3-phosphate dehydrogenase; GC, gastric cancer; TCGA, Cancer Genome Atlas-Stomach Adenocarcinoma; GEPIA, gene expression profiling interactive analysis; GSEA, gene set enrichment analysis; GSK3β, glycogen synthase kinase 3 beta; H3, histone 3; HA, hemagglutinin; H&E, hematoxylin and eosin; hFAST, human Fas-activated serine/threonine kinase; hnRNP K, heterogeneous nuclear ribonucleoprotein K; HOXA11-AS, homeobox A11 antisense RNA; HR, hazard ratio; IF, immunofluorescence; IgG, immunoglobulin G; IHC, immunohistochemical; IP, immunoprecipitation; lncRNA, long non-coding RNA; MMP7, matrix metallopeptidase 7; NT, non-target; OC, ovarian cancer; OS, overall survival; PVT-1, Pvt1 oncogene; RACE, rapid amplification of cDNA ends;; RIP, RNA Immunoprecipitation; RT-qPCR, quantitative real-time polymerase chain reaction; SDCBP2, syndecan binding protein 2; SDCBP2-AS1, SDCBP2 antisense RNA 1; SDS-PAGE, sodium dodecyl sulfate-polyacrylamide gel electrophoresis; SLCO4A1-AS1, solute carrier organic anion transporter family member 4A1 antisense RNA 1; SNHG5, small nucleolar RNA host gene 5; SUMO-1, small ubiquitin-like modifier 1; UCA1, urothelial cancer associated 1.

Jing Han, Menglin Nie and Cong Chen contributed equally to this work.

were conducted to clarify the interactions of SDCBP2-AS1 and heterogeneous nuclear ribonucleoprotein (hnRNP) K. RNA-sequencing, immunoprecipitation, immunofluorescence, and luciferase analyses were performed to investigate the functions of SDCBP2-AS1.

Results: SDCBP2-AS1 was significantly downregulated in GC tissues and predictive of poor patient prognosis. Silencing of SDCBP2-AS1 promoted the proliferation and migration of GC cells both in vitro and in vivo. Mechanically, SDCBP2-AS1 physically bound to hnRNP K to repress SUMOylation of hnRNP K and facilitated ubiquitination of hnRNP K and β-catenin, thereby promoting the degradation of β-catenin in the cytoplasm. Silencing of SDCBP2-AS1 caused SUMOylation of hnRNP K and stabilized β-catenin activity, which altered transcription of downstream genes, resulting in tumorigenesis and metastasis of GC. Moreover, the knockdown of hnRNP K partially abrogated the effects of SDCBP2-AS1.

Conclusions: SDCBP2-AS1 interacts with hnRNP K to suppress tumorigenesis and metastasis of GC and regulates post-transcriptional modifications of hnRNP K to destabilize β-catenin. These findings suggest SDCBP2-AS1 as a potential target for the treatment of GC.

KEYWORDS

SDCBP2-AS1, gastric cancer, hnRNP K, β-catenin, post-transcriptional modifications, tumorigenesis

1 | BACKGROUND

Gastric cancer (GC) is a major cause of cancer-related death worldwide, although its incidence varies across different geographical regions [1, 2]. Despite standardized treatments have improved patients survival in the last decade, the 5-year survival rate remains low [3]. Early detection can largely promote the 5-year survival rate; however, due to the lack of effective diagnostic and therapeutic strategies, more than 80% GC patients in China had advanced diseases at the time of diagnosis, and the 5-year survival rate is less than 20% [4, 5]. Hence, novel biomarkers and therapeutic targets are urgently needed for the diagnosis and prognosis prediction of GC to reduce mortality.

Long non-coding RNAs (lncRNAs) are important RNA transcripts longer than 200 nucleotides with limited or no protein-coding capacity [6, 7]. lncRNAs are crucial to various biological processes, especially tumorigenesis and metastasis [8–11]. However, the specific molecular pathogenic mechanisms of lncRNAs underlying the initiation and progression of GC remain unclear.

Wnt/β-catenin signaling controls several fundamental cell functions, such as proliferation, differentiation, migration, and stemness. It therefore plays a critical role in the gastrointestinal epithelial homeostasis. Even for GC, a highly heterogeneous disease with phenotypic diversity, the dysregulation of Wnt/β-catenin signaling pathway still has been observed in approximately 50% of GC patients [12, 13]. β-catenin, the prime effecter of canonical Wnt signaling, contributes to tumor progression by enhancing the proliferation and invasiveness of GC cells [14, 15]. Activation of the canonical Wnt/β-catenin signaling pathway is dependent on controlling the accumulation of β-catenin in the cytoplasm and its translocation into the nucleus to regulate the transcription of downstream genes. Regulation of cytoplasmic β-catenin is controlled by targeting phosphorylated β-catenin to the proteosomes for degradation via E3 ubiquitin ligase, resulting in low concentrations of cytoplasmic β-catenin [16]. However, the relative importance of temporal activation of β-catenin and its crosstalk with lncRNAs is not well understood.

Our group has previously identified a collection of candidate lncRNAs, including syndecan-binding protein 2-antisense RNA 1 (SDCBP2-AS1), involved in the GC progression [17]. In continuation, the present study aimed to investigate the molecular mechanism of SDCBP2-AS1 in mediating the transcription, stability, and transactivation of β-catenin in the development of GC and to explore potential prognostic implications.

TABLE 1 Associations between SDCBP2-AS1 expression levels and clinicopathological features of GC patients

Characteristic	Total [cases (%)]	Expression of SDCBP2-AS1 [cases (%)]		P
		Low	High	
Total	**132**	**73 (55.3)**	**59 (44.7)**	
Gender				0.019
Male	88 (66.7)	55 (62.5)	33 (37.5)	
Female	44 (33.3)	18 (40.9)	26 (59.1)	
Age (years)				0.145
≤60	69 (52.3)	34 (49.3)	35 (50.7)	
>60	63 (47.7)	39 (61.9)	24 (38.1)	
Tumor location				0.748
Cardiac	34 (25.8)	18 (52.9)	16 (47.1)	
Non-cardiac	98 (74.2)	55 (56.1)	43 (43.9)	
Tumor diameter				0.016
≤4 cm	63 (47.7)	28 (44.4)	35 (55.6)	
>4 cm	69 (52.3)	45 (65.2)	24 (34.8)	
Pathological type				0.033
Adenocarcinoma	103 (78.0)	62 (60.2)	41 (39.8)	
Signet-ring cell carcinoma and others	29 (22.0)	11 (37.9)	18 (62.1)	
Histologic differentiation				0.077
Well or moderate	67 (50.8)	32 (47.8)	35 (52.2)	
Poor	65 (49.2)	41 (63.1)	24 (36.9)	
Vascular invasion				0.293
Absent	56 (42.4)	28 (50.0)	28 (50.0)	
Present	76 (57.6)	45 (59.2)	31 (40.8)	
Depth of invasion				0.137
T1-2	22 (16.7)	9 (40.9)	13 (59.1)	
T3-4	110 (83.3)	64 (58.2)	46 (41.8)	
Lymphatic metastasis				<0.001
No	31 (23.5)	7 (22.6)	24 (77.4)	
Yes	101 (76.5)	66 (65.3)	35 (34.7)	
Distant metastasis				0.036
M0	123 (93.2)	65 (52.8)	58 (47.2)	
M1	9 (6.7)	8 (88.9)	1 (11.1)	
pTNM stage				<0.001
I-II	55 (41.7)	20 (36.4)	35 (63.6)	
III-IV	77 (58.3)	53 (68.8)	24 (31.2)	

Abbreviations: SDCBP2-AS1, syndecan binding protein 2 antisense RNA 1; GC, gastric cancer.

2 | MATERIALS AND METHODS

2.1 | Clinical samples

A total of 132 GC tumor tissues and paired adjacent normal tissues were obtained from GC patients via radical resection conducted at the Peking University Cancer Hospital (Beijing, China) between January 2007 and December 2010. None of the patients received chemotherapy or radiotherapy before surgery, and all were followed up until March 2016. All subjects provided informed consent for the use of specimens in this study. The study protocol was approved by the Ethics Committee of Peking University Cancer Hospital (approval number: 2018KT07) and conducted in accordance with the ethical principles for medical research involving human subjects described in the Declaration of Helsinki. After resection, the tissues were snap-frozen in liquid nitrogen and then stored at −80°C prior to RNA extraction. Detailed information of the patients is provided in Table 1. The

tumor-node-metastasis (TNM) stage of GC was determined in accordance with the Cancer Staging Manual of the American Joint Committee on Cancer (8th edition). Overall survival (OS) was calculated from the date of surgery to the date of death due to any reason, while disease-free survival (DFS) was defined as the duration from the date of surgery to the date of death or recurrence of any complications during follow-up. Patients without an endpoint (progression or death) were censored at the date of the last follow-up.

2.2 | Databases and bioinformatics analysis

The coding potential of SDCBP2-AS1 was analyzed using the online tools Open Reading Frame Finder (https://www.ncbi.nlm.nih.gov/orffinder/), Coding Potential Calculator 2 (http://cpc2.gao-lab.org/), Coding-Potential Assessment Tool (http://lilab.research.bcm.edu/cpat/), and LNCipedia (https://lncipedia.org/) [18–21]. Gene Expression Profiling Interactive Analysis (GEPIA) web tool (http://gepia.cancer-pku.cn/) and Asian Cancer Research Group databases (https://consortiapedia.fastercures.org/consortia/acrg/) were used to analyze the correlation between SDCBP2-AS1 and SDCBP2 expression in GC samples. Kaplan-Meier survival plot of DFS and OS of GC patients in the dataset GSE22377 (http://www.ncbi.nlm.nih.gov/geo/geo2r/?acc=GSE22377) was analyzed by the web tool Kaplan-Meier Plotter (http://kmplot.com/analysis/index.php?p=service&cancer=gastric) [22].

2.3 | Cell cultures

Human embryonic kidney 293 (HEK293T) cells and human gastric adenocarcinoma hyperdiploid (AGS) cells were obtained from the American Type Culture Collection (Manassas, VA, USA). GC cells (BGC823, SGC7901, MGC803, HGC27, and N87) and normal gastric epithelial (GES-1) cells were obtained from the Shanghai Cell Research Institute (Chinese Academy of Sciences, Shanghai, China). Well-differentiated human gastric adenocarcinoma (MKN28) cells were obtained from the Japanese Collection of Research Bioresources Cell Bank (National Institutes of Biomedical Innovation, Health and Nutrition, Osaka, Japan). All cell lines, which were obtained between 2014 and 2015 and authenticated by short tandem repeat profiling, were cultured in Dulbecco's modified Eagle's medium (DMEM) (Gibco; Invitrogen Corporation, Carlsbad, CA, USA) supplemented with 10% fetal bovine serum (Gibco) and maintained at 37°C in 5% CO_2 as previously described [23]. Cells were incubated in serum-free medium and treated with cycloheximide (CHX) (Sigma-Aldrich Pty. Ltd., Merck KGaA, Darmstadt, Germany) for 4 h or MG132 (Sigma-Aldrich) for 8 h as indicated. Routine testing for *Mycoplasma* contamination was performed using polymerase chain reaction (PCR). Cells were grown for no more than 20 passages prior to experimentation.

2.4 | Plasmid construction and establishment of stable cell lines

Full-length cDNA of human SDCBP2-AS1 (2479 bp) was synthesized by Invitrogen Corporation and cloned into the expression vector pcDNA3.0. A series of SDCBP2-AS1 deletion mutants were designed according to the secondary structure of SDCBP2-AS1 predicted from the RNAfold Web Server (http://rna.tbi.univie.ac.at/). Truncations of SDCBP2-AS1 were amplified with appropriate primer sets and subcloned into plasmid pcDNA3.0. Human hnRNP K cDNA (1395 bp) was amplified from GC tissues and subcloned into plasmid p3XFLAG-CMV-10 (Sigma-Aldrich). Truncations of hnRNP K were amplified with appropriate primer sets and subcloned into plasmid p3XFLAG-CMV-10. The hnRNP K K422R mutant was created with the restriction enzyme *Dpn*I and subcloned into plasmid p3XFLAG-CMV-10. Each mutation was verified against the whole hnRNP K cDNA sequence. Human small ubiquitin-like modifier 1 (SUMO-1) cDNA was amplified from GC tissues and subcloned into plasmid pCMV-HA. HA-catenin beta 1 (CTNNB1) was subcloned into vector GV366 (Shanghai Genechem Co., Ltd., Shanghai, China). The final construct was verified by sequencing. Stable SDCBP2-AS1-overexpressing SGC7901 cell line were generated and screened by administration of neomycin (Invitrogen Corporation). Small hairpin RNA (shRNA) against SDCBP2-AS1 was provided by Invitrogen Corporation, and shRNA against hnRNP K was obtained from Shanghai Genechem Co., Ltd. Stable SDCBP2-AS1-knockdown BGC823 and MKN28 cells and hnRNP K-knockdown SGC7901 cells were established with a lentiviral vector in accordance with the manufacturer's instructions. All primers and shRNA sequences are listed in Supplementary Table S1. GC cells were transfected with plasmid vectors or lentiviruses encoding shRNAs using DNA Miniprep Kits [Tiangen Biotech (Beijing) Co. Ltd., Beijing, China] and Lipofectamine 2000transfection reagent (Invitrogen Corporation) following the manufacturer's instructions and screened by administration of puromycin (Invitrogen Corporation). Plasmid p3XFLAG-CMV-10 or the empty vector pCMV-HA was used as an overexpression control (Con), while non-target (NT) shRNA was used as a knockdown control.

2.5 | RNA extraction and quantitative real-time PCR (RT-qPCR)

Total RNA was extracted from the tissue samples and cell lines using TRIzol reagent (Invitrogen Corporation) in accordance with the manufacturer's instructions, and reversely transcribed into complementary DNA using a reverse transcription system kit (Invitrogen Corporation) with the ABI PRISM 7500 Sequence Detection System (Applied Biosystems, Foster City, CA, USA) and the SYBR Green method (amplification condition: 95°C for 10 min, followed by 40 cycles at 95°C for 15 s and 60°C for 1 min). For each sample, gene expression was normalized to glyceraldehyde 3-phosphate dehydrogenase (GAPDH) or U6. The primer sequences used for RT-qPCR are listed in Supplementary Table S1. Each RT-qPCR reaction was performed in triplicate, and relative RNA expression was calculated using the $2^{-\Delta\Delta Ct}$ method.

2.6 | Rapid amplification of cDNA ends (RACE)

RACE was performed using the SMARTer 5′/3′ RACE kit (Takara Bio Inc., Shiga, Japan) in accordance with the manufacturer's recommendations. Briefly, first-strand cDNA was synthesized with SMARTScribe™ Reverse Transcriptase (RT) and a modified oligo (dT) primer that contained an additional sequence as a primer binding site for downstream 3′ PCR reactions. The SMARTer II A Oligonucleotide, which contained several non-template residues, was annealed to the 5′-end as an additional template for SMARTScribe RT and as a primer binding site for downstream 5′ PCR reactions. The 5′ and 3′ RACE reactions were performed by PCR with the SDCBP2-AS1-specific primer pair SDC5′GSP1/SDC3′GSP1 and the universal primer UPM long (Supplementary Table S1).

2.7 | Cell proliferation and colony formation assays

GC cells (3000 cells/well) with stable knockdown of endogenous SDCBP2-AS1 (BGC823 and MKN28) or stable ectopic expression of SDCBP2-AS1 (SGC7901) were seeded into 96-well plates, and cell proliferation was monitored with an IncuCyte® Live-Cell Analysis System (Essen Bio-Science, Ann Arbor, MI, USA). For the colony formation assay, the established stable cell lines were seeded into 6-well plates at 600 cells/well and incubated at 37°C in 5% CO_2 for 14 days. Afterward, they were carefully washed twice with phosphate-buffered saline, fixed with 75% ethyl alcohol for 15 min at 21°C, and stained with 0.1% crystal violet. Washing out the dye and drying, the plates were photographed. The ImageJ software (National Institutes of Health, Bethesda, MD, USA) was used to quantify the colonies containing ≥50 cells objectively.

2.8 | Migration and invasion assays and wound-healing assay

Transwell chambers with and without a Matrigel matrix (Corning Life Science, Woburn, MA, USA) were used to examine cell migration and invasion, respectively. Cells (3 $\times 10^4$) were suspended in 200 μL of serum-free DMEM and seeded onto polycarbonate filters, which were either pre-coated with 100 μL of Matrigel for the invasion assay or left uncoated for the migration assay. The lower chamber was loaded with 600 μL of DMEM containing 10% fetal bovine serum.

The wound-healing assay was performed to assess cell motility. Briefly, wounds were generated by scratching monolayers of cells at 100% confluence using a 200-μL plastic pipette tip. The growth medium was replaced with serum-free medium, and the wounds were monitored in real-time with an IncuCyte® Live-Cell Analysis System.

2.9 | In vivo tumorigenicity and metastasis assays

Female BALB/c nude mice (age, 4-6 weeks; body weight, 18-20 g; Charles River, Beijing, China) were subcutaneously injected via the left and right flanks with 5 $\times$ 10^6 SDCBP2-AS1-knockdown BGC823 cells or SDCBP2-AS1-overexpressing SGC79901 cells. NT BGC823 cells and Con SGC79901 cells were used as controls. Approximate tumor volume (mm^3) was calculated according to the formula [(smallest diameter^2 $\times$ widest diameter)/2] as previously described [24]. After 3 weeks, mice were euthanized by CO_2 inhalation, and the tumors were harvested and immediatelyweighted.

A lung metastasis model was created using female BALB/c nude mice that were subcutaneously injected via the tail vein with 2 $\times 10^6$ SDCBP2-AS1-knockdown BGC823 cells or SDCBP2-AS1-overexpressing SGC7901 cells. At 4 weeks post-injection, all mice were euthanized by CO_2 inhalation, and the lungs were collected and fixed with Bouin's solution via injection through the main bronchi. The tissue samples were photographed, and metastases were evaluated and finally embedded in paraffin.

Generally, body weight loss of more than 20% of the pre-procedural weight or the size of the subcutaneous tumors reaching 20 mm was considered as a humane end-point. All animal procedures were conducted following the

guidelines of the Laboratory Animal Ethics Committee of Beijing Cancer Hospital (EAEC 2019-03).

2.10 | Immunohistochemical (IHC) analysis

Generally, all dissected tissues were formalin-fixed and paraffin-embedded for staining with hematoxylin and eosin (H&E) and IHC analysis. As previously described [19], the slides were dewaxed and gradually hydrated. After retrieving antigens by using citrate buffer (Sigma-Aldrich) at 120°C for 3 min and incubating within 3% H_2O_2 to eliminate endogenous enzymes, the slides were incubated overnight at 4°C with antibodies against Ki-67, hnRNP K, and β-catenin (Supplementary Table S2). Antigen visualization was performed with ImmPRESS Peroxidase Polymer Detection Reagent (Vector Laboratories, Burlingame, CA, USA) and 3,3′-diaminobenzidine, followed by counterstaining with Mayer's hematoxylin (Sigma-Aldrich). The stained specimens were viewed under a light microscope (Nikon Corporation, Tokyo, Japan). For Ki-67, the proportion of positively stained cells was calculated. For β-catenin, the scores of 0 (negative), 1 (weak), 2 (medium), and 3 (strong) were used for staining intensity quantification, while the scores of 0 (<5%), 1 (5%–25%), 2 (26%–50%), 3 (51%–75%) and 4 (>75%), which were based on the percentage of the positive staining areas in relation to the whole cancerous area, were used to evaluate the extent of staining. Then, the final IHC score was calculated by multiplying scores of staining intensity and percentage of positivity. Cases with a final staining score of ≤4 were deemed as low expression, and those with a score of >4 were reckoned as high expression. All slides were evaluated independently by two pathologists, who were blinded to the patients' data and clinical outcomes.

2.11 | RNA-fluorescence in situ hybridization (FISH) and subcellular fractionation

RNA-FISH with a digoxin-labeled RNA probe (Supplementary Table S3) was used to detect the subcellular location of SDCBP2-AS1 as previously described [24]. Briefly, the nuclei were labeled with 4′,6-diamidino-2-phenylindole (blue), and SDCBP2-AS1 was labeled with a cyanine 3-conjugated RNA probe (red). Images were captured using an LSM 800 confocal microscope (Carl Zeiss AG, Jena, Germany). To separate the nuclear and cytoplasmic fractions, RNA was isolated from BGC823 and SGC7901 cells using a PARIS™ kit (AM1921, Life Technologies, Carlsbad, CA, USA) in accordance with the manufacturer's instructions. SDCBP2-AS1 RNA expres-

sion levels in the nuclear and cytoplasmic fractions were determined by RT-qPCR. U6 and GAPDH were used as positive controls for the nuclear and cytoplasmic fractions, respectively. The primer sequences are listed in Supplementary Table S1.

2.12 | RNA pull-down assay and mass spectrometry

The RNA pull-down assay was performed using the Pierce Magnetic RNA-Protein Pull-Down Kit (20164, Thermo Fisher Scientific, Rockford, IL, USA) in accordance with the manufacturer's instructions. Briefly, the sense or antisense SDCBP2-AS1 sequence was transcribed in vitro with a biotin RNA-labeling mix and T7 RNA polymerase (Invitrogen Corporation) in accordance with the manufacturer's instructions. The positive control, negative control, biotinylated SDCBP2-AS1 or antisense SDCBP2-AS1 was incubated with streptavidin-linked magnetic beads and total BGC823 cell lysates at 21°C for 2 h. After washing the bead-RNA-protein complexes four times with binding/washing buffer, the proteins were precipitated and diluted in the protein lysis buffer. The collected proteins were separated by electrophoresis for one-shot mass spectrometry or Western blotting analysis. Pull-down samples harvested from immunoprecipitation were separated with sodium dodecyl sulfate-polyacrylamide gel electrophoresis (SDS-PAGE) and stained with Pierce Silver Stain Kit (24612, Thermo Fisher Scientific) according to the instruction manual. The specific strip was cut for mass spectrometry. The primers used for in vitro transcription are listed in Supplementary Table S1 and the antibodies in Supplementary Table S2. Mass spectrometry was performed at the Institute of Biotechnology of the Peking University Health Science Center (Beijing, China).

2.13 | RNA immunoprecipitation (RIP)

RIP assays were performed using the Magna RIP RNA-Binding Protein Immunoprecipitation Kit (17-700, EMD Millipore Corporation, Billerica, MA, USA), as previously described [24]. Briefly, 1×10^7 GC cells were harvested and lysed with RIP lysis buffer, and the cell extract was incubated with magnetic beads conjugated with antibodies against hnRNP K or normal rabbit immunoglobulin G (IgG) as a control (Supplementary Table S2). Afterward, the beads were washed and then incubated with proteinase K (EO0491, Thermo Fisher Scientific) to remove proteins. The retrieved RNA was amplified by RT-qPCR using primers specific for SDCBP2-AS1 (Supplementary Table S1). Total RNA (as input controls) and normal

IgG controls were assayed simultaneously to verify the RT-qPCR results.

2.14 | Western blotting analysis

The proteins isolated from the tissue samples and cell lines were separated by electrophoresis and transferred to polyvinylidene fluoride membranes, which were probed with primary antibodies against matrix metallopeptidase 7 (MMP7), cyclin D1, c-Myc, β-catenin, phospho-β-catenin (Ser33/37/Thr41), glycogen synthase kinase 3 beta (GSK3β), Axin1, adenomatous polyposis coli (APC), histone 3 (H3), Wnt5a, hnRNP K, ubiquitin, Wnt3a, GAPDH, hemagglutinin (HA), and Flag. All antibodies are listed in Supplementary Table S2.

2.15 | RNA-sequencing (RNA-seq)

Total RNA was isolated from 1×10^6 BGC823 cells with or without stable SDCBP2-AS1 using the TRizol reagent. Sequence libraries were generated using the TruSeq® RNA Sample Preparation Kit (Illumina, Inc., San Diego, CA, USA) in accordance with the manufacturer's recommendations. Transcriptome sequencing was performed using an Illumina HiSeq X-Ten platform by Novogene Biotech Co., Ltd. (Beijing, China). Fragments per kilo-base of transcript per million fragments mapped of each gene were calculated, and differentially expressed genes (fold change > 2.0, $P < 0.01$, false discovery rate < 0.05) were selected for gene set enrichment analysis (GSEA), which was performed using GSEA software (v4.0.3; https://www.gsea-msigdb.org/gsea/index.jsp).

2.16 | Immunofluorescence (IF) assay

The cells were fixed to the chamber slide with 4% formaldehyde solution, and the cell membranes were penetrated by the addition of 1% Triton X-100. Normal sheep serum (Dako A/S, Glostrup, Denmark) was used to block the cells at 21°C for 30 min. Afterward, the cells were probed with an antibody against β-catenin at 4°C for 12-16 h, followed by a secondary Alexa Fluor™ 594 antibody for IF staining. After Hoechst staining, the cells were observed with an LSM 800 confocal microscope.

2.17 | TOP/FOP-flash luciferase reporter analysis

As previously described [25], the TOP/FOP-flash luciferase reporter assay was applied to analyze the activity of the Wnt/β-catenin signaling pathway. GC cells were seeded into 48-well plates (6×10^4 cells/well) and transiently co-transfected with 250 ng of TOP-FLASH or FOP-FLASH and 25 ng of the plasmid pRL-SV40. Luciferase activity was measured with the Dual-Luciferase Reporter Assay System (E1910, Promega Corporation, Madison, WI, USA) in accordance with the manufacturer's protocol. The TOP/FOP ratio was calculated as an indicator of β-catenin signaling activity. Each experiment was performed in triplicate and repeated at least three times.

2.18 | Immunoprecipitation (IP)

IP was performed as previously described [26] with antibodies specific for hnRNP K, β-catenin, FLAG, or HA. The cells were transfected as indicated and harvested with IP lysis buffer (20 mmol/L Tris-HCl at pH 7.5, 150 mmol/L NaCl, 1 mmol/L ethylenediaminetetraacetic acid, 0.1% NP-40 nonionic detergent, 10% glycerol [vol/vol], 1 mmol/L dithiothreitol, protease inhibitor cocktail). The lysates were rotated at 4°C for 1 h and centrifuged at 12,000 rpm for 15 min. Then, the supernatants were collected and incubated overnight at 4°C with the appropriate antibody or an isotype-matched antibody against IgG. After washing once with lysis buffer and twice with lysis buffer without 1% NP-40 to remove all unbound proteins, the precipitants and lysates were subjected to Western blotting analysis with appropriate antibodies.

2.19 | Statistical analysis

The cutoff value of RT-qPCR results was determined by survival significance analysis using the tool Cutoff Finder (http://molpath.charite.de/cutoff/) [27]. Kaplan-Meier curves were constructed to assess survival, and the log-rank test was used to compare survival rates between groups. The chi-square test was used to identify the association between SDCBP2-AS1 expression levels and clinicopathological features of GC patients. A multivariate Cox proportional hazards model was used to assess the effects of variables, including SDCBP2-AS1, on survival using IBM SPSS Statistics for Windows, version 22.0. (IBM Corporation, Armonk, NY, USA). The Pearson's correlation test was used to identify correlations between the expression levels of SDCBP2-AS1 and β-catenin. For functional analysis, data are presented as the mean ± standard deviation (SD). Comparisons between two and among three or more groups were conducted using the two-tailed Student's t-test and analysis of variance, respectively, with GraphPad Prism 7 software (GraphPad Software Inc., La Jolla, CA, USA). All experiments were performed at least

three times. A *P* value of <0.05 was considered statistically significant.

3 | RESULTS

3.1 | Downregulation of SDCBP2-AS1 in GC tissues was indicative of poor outcomes

Based our previous study [17], several lncRNAs were found to be significantly related to the progression of GC, one of which was SDCBP2-AS1. SDCBP2-AS1 was identified as a novel gene, and therefore, was the focus of the present study. The results of 5′/3′ RACE identified the novel lncRNA transcript as SDCBP2-AS1 (NCBI reference sequence: NR_040047.1) (Supplementary Figure S1A). SDCBP2-AS1 was conserved among primates (Supplementary Figure S1B) and was confirmed as a noncoding gene using the online tools (Supplementary Figure S1C-F). SDCBP2-AS1 is located at chromosome 20p13 and overlaps with a short length of the 3' untranslated regions of the gene encoding SDCBP2 on the opposite DNA strand (Supplementary Figure S1B). Searches of The Cancer Genome Atlas-Stomach Adenocarcinoma (TCGA) GC database from GEPIA web and Asian Cancer Research Group databases confirmed that there was no correlation between SDCBP2 and SDCBP2-AS1 at the posttranscriptional level (Supplementary Figure S1G). Hence, SDCBP2-AS1 was confirmed as a novel lncRNA.

Next, potential associations between SDCBP2-AS1 expression and different clinicopathological features of our clinical samples were investigated. The results showed that SDCBP2-AS1 expression was significantly decreased in GC tissues as compared with the matched adjacent non-tumor tissues (Figure 1A-B). Based on the cutoff value of SDCBP2-AS1 (0.0058), obtained from the Cutoff Finder, the patients were divided into SDCBP2-AS1 high-expression (*n* = 59) and low-expression groups (*n* = 73). Notably, low expression of SDCBP2-AS1 was associated with adenocarcinoma (*P* = 0.033), larger tumor size (*P* = 0.016), lymph node metastasis (*P* < 0.001), distant metastasis (*P* = 0.036), and advanced pathological TNM (pTNM) stage (*P* < 0.001) in GC patients (Table 1). Kaplan-Meier survival analysis showed that the DFS and OS rates of the low SDCBP2-AS1 group were lower than those of the high SDCBP2-AS1 group (Figure 1C). Univariate and multivariate analyses indicated that SDCBP2-AS1 expression was an independent prognostic factor for GC (Table 2). To validate these findings, the Kaplan-Meier plotter was used to explore potential associations between SDCBP2-AS1 overexpression and survival using the dataset GSE22377. The results showed that lower expression of SDCBP2-AS1 was related to shorter OS and DFS (Figure 1D). These findings verified that low expression of SDCBP2-AS1 was predictive of a poor prognosis for GC patients. Further in vitro evaluation revealed that SDCBP2-AS1 expression was higher in normal GES-1 cells than in GC cell lines (Supplementary Figure S1H).

3.2 | SDCBP2-AS1 suppressed proliferation and metastasis of GC cells in vitro

SDCBP2-AS1 was knocked-down in BGC823 and MKN28 cells using two shRNAs. SDCBP2-AS1 was overexpressed in SGC7901 cells. RT-qPCR analysis was used to determine the efficacy of transfection (Supplementary Figure S2A-B). Notably, SDCBP2 mRNA expression was independent of SDCBP2-AS1 expression in GC cell lines with SDCBP2 wild-type, knockdown or overexpression (Supplementary Figure S2C-E). The cell proliferation and colony formation assays demonstrated that knockdown of SDCBP2-AS1 significantly promoted the proliferation and colony formation in both cell lines (Figure 2A-B), whereas overexpression of SCBP2-AS1 had opposite effects (Figure 2C-D). Further, the effects of SDCBP2-AS1 on metastasis of GC cells were explored. The results of the transwell and wound-healing assays showed that silencing of SDCBP2-AS1 increased the migration and invasion of BGC823 and MKN28 cells (Figure 2E-F), while overexpression of SDCBP2-AS1 enhanced the mobility of SGC7901 cells (Figure 2G-H). These in vitro data indicate that knockdown of SDCBP2-AS1 aggressively promoted proliferation, migration, and invasion of GC cells.

3.3 | SDCBP2-AS1 suppressed growth and metastasis of GC cells in vivo

The influence of SDCBP2-AS1 on the tumorigenic and metastatic capacities of GC cells was determined using in vivo xenograft tumor and lung metastasis models in nude mice. The xenograft tumor model was established by subcutaneous injection of BGC823 cells stably transfected with shSDCBP2-AS1#1 (sh1) or the NT control. The resulting tumors were visibly larger and exhibited faster growth in the sh1 group than in the NT group (Figure 3A-C). This difference was further confirmed by staining with H&E and IHC analysis of Ki-67, which showed that Ki-67 expression in tumor tissues was significantly increased in the sh1 group as compared with the NT group (Figure 3D). Moreover, a lung metastasis model showed that the NT group had fewer metastatic lesions than the sh1 group (Figure 3E-F). This difference was further confirmed by staining the lung tissue sections with
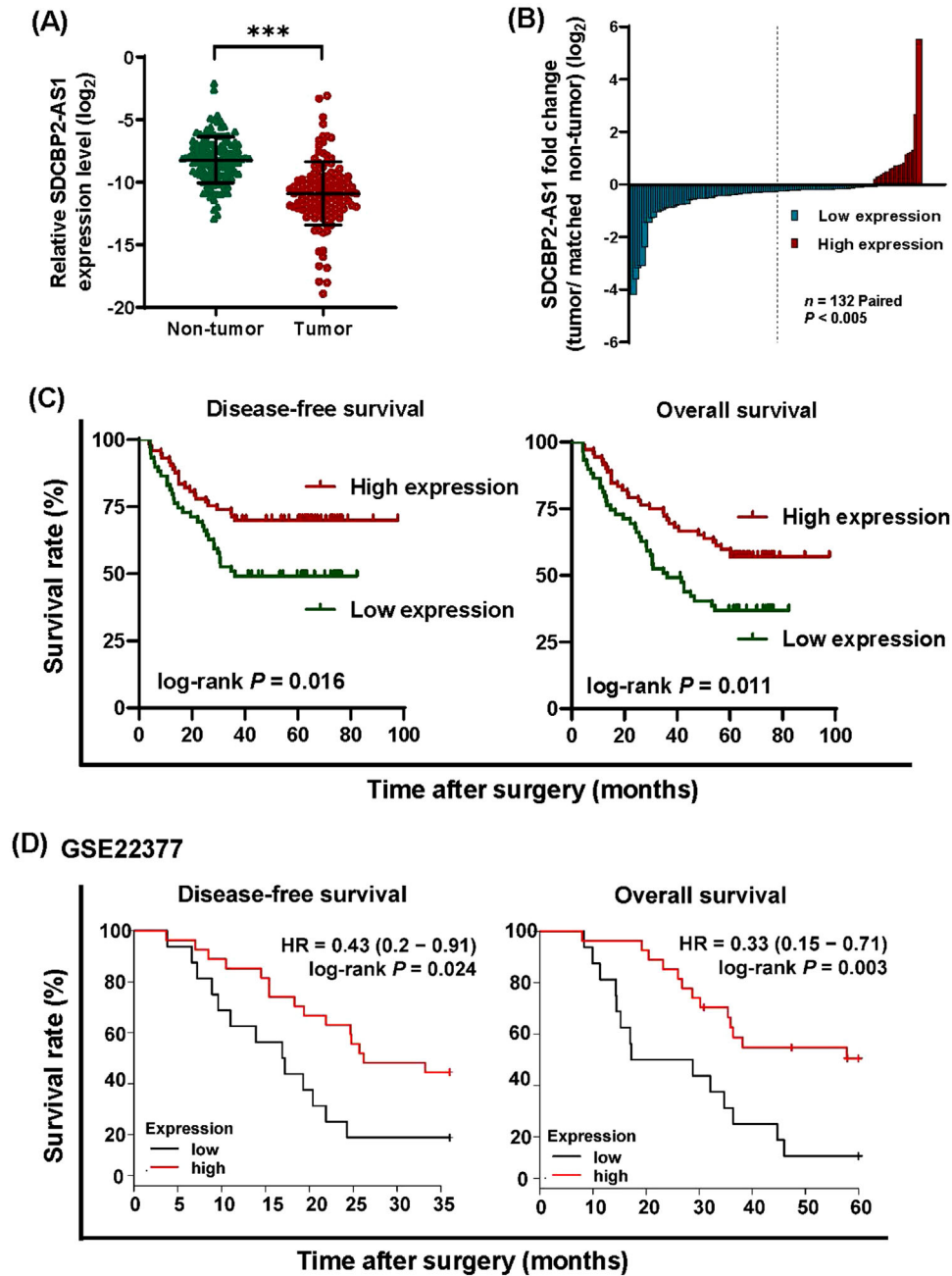
FIGURE 1 SDCBP2-AS1 was downregulated in GC tissues and indicated poor patient outcomes. (A) SDCBP2-AS1 expression was examined by RT-qPCR in GC and non-tumor tissues from 198 patients. (B) Fold-changes in SDCBP2-AS1 expression in paired GC tissues (normalized to adjacent non-normal tissues) from 132 patients. Vertical dotted line represents the median number of samples. (C) Kaplan-Meier survival analysis of DFS and OS of the 132 patients according to SDCBP2-AS1 levels in GC tissues. (D) Kaplan-Meier survival analysis of DFS and OS according to SDCBP2-AS1 levels in GC tissues by mining a public microarray dataset GSE22377 ($n = 43$). Data are presented as the mean $\pm$ SD of three independent experiments. ***$P < 0.001$. Abbreviations: SDCBP2-AS1, syndecan binding protein 2 antisense RNA 1; GC, gastric cancer; RT-qPCR, quantitative real-time polymerase chain reaction; DFS, disease-free survival; OS, overall survival; HR, hazard ratio; SD, standard deviation

H&E and IHC analysis of Ki-67 (Figure 3G). Meanwhile, SDCBP2-AS1 overexpression decreased the tumorigenic and metastatic capacity of SGC7901 cells (Supplementary Figure S3). Taken together, these in vivo results support the tumor-suppressive role of SDCBP2-AS1 in GC.

3.4 | SDCBP2-AS1 interacted with hnRNP K in the cytoplasm

To identify potential mechanisms, the distribution of SDCBP2-AS1 in GC cells was investigated using

TABLE 2 Univariate and multivariate analyses for overall survival prognostic parameters in GC patients

Characteristic	Univariate analysis			Multivariate analysis		
	HR	95% CI	*P*	HR	95% CI	*P*
Gender (male vs. female)	1.326	0.780-2.253	0.298	0.792	0.469–1.160	0.248
Age (≤60 vs. >60 years)	1.036	0.644-1.666	0.885	1.092	0.371-3.820	0.646
Tumor location (cardiac vs. noncardiac)	0.713	0.426-1.193	0.198			
Tumor size (≤ 5cm vs. > 5cm)	1.910	1.170-3.118	0.010	1.429	0.841-2.428	0.187
Pathological types (adenocarcinoma vs. others)	0.911	0.506-1.640	0.756			
pTNM stage (I-II vs. III-IV)	1.907	1.139-3.192	0.014	1.172	0.416–1.785	0.046
Histologic differentiation (well or moderate vs. poor)	1.161	0.721-1.869	0.540			
Vascular invasion (absent vs. present)	2.400	1.422-4.048	0.001	2.139	1.231-3.717	0.007
Depth of invasion (T1-2 vs. T3-4)	3.295	1.324-8.198	0.010			
Lymphatic metastasis (no vs. yes)	2.155	1.100-4.221	0.025			
Distant metastasis (M0 vs. M1)	6.951	3.365-14.359	<0.001			
SDCBP2-AS1 expression (low vs. high)	0.479	0.288-0.798	0.005	0.547	0.318–0.944	0.030

Abbreviations: SDCBP2-AS1, syndecan binding protein 2 antisense RNA 1; GC, gastric cancer; HR, hazard ratio; CI, confidence interval.

RNA-FISH and RNA subcellular fractionation. The results showed that SDCBP2-AS1 was more prevalent in the cytoplasm (Figure 4A-B). Further, the RNA pull-down assay with biotinylated SDCBP2-AS1 was employed to identify the protein partner of SDCBP2-AS1. The retrieved proteins were separated by electrophoresis and subjected to silver staining. Finally, several differential bands were selected for mass spectrometry (Supplementary Table S4), which confirmed that hnRNP K interacted with SDCBP2-AS1 but not antisense SDCBP2-AS1 (Figure 4C-D). Next, in vivo RIP analysis showed that hnRNP K interacted with SDCBP2-AS1 in BGC823 cells (Figure 4E). Collectively, these findings demonstrated the interplay between SDCBP2-AS1 and hnRNP K. To determine which regions of SDCBP2-AS1 bind to hnRNP K, a series of SDCBP2-AS1 deletion mutants was constructed according to the predicted secondary structure of SDCBP2-AS1 (Figure 4F). RNA fragments were in vitro transcribed from the deletion constructs for the RNA pull-down assay (Figure 4G). Immunoblot analysis of hnRNP K in protein samples pulled down by different SDCBP2-AS1 RNA fragments showed that RNA fragments with deletions of nucleotide 541-2479 completely lost the ability to bind to hnRNP K (Figure 4H). The sequence of Exon 2 could interact with hnRNP K, its RNA secondary structure was totally different from the full-length sequence of SDCBP2-AS1 though (Supplementary Figure S4). Thus, the Exon 3 sequence was determined to be essential for the interaction between SDCBP2-AS1 and hnRNP K (Figure 4H). Furthermore, hnRNP K harbors several functional domains that participate in RNA-protein interactions, reportedly involving three K homology (KH) domains (KH1, KH2, and KH3).

However, the KI domain, located between the KH2 and KH3 domains, mediates hnRNP K activity, although the underlying mechanism remains unclear [28]. The RIP assay with a series of Flag-tagged hnRNP K deletion mutants in BGC823 cells (Figure 4I-J) indicated that KH3 had the greatest ability to bind to SDCBP2-AS1, while there was no significant difference in the capacities of the other domains to interact with SDCBP2-AS1 (Figure 4K). These results identified the specific regions of SDCBP2-AS1 with the ability to bind to the hnRNP K protein domains in GC cells.

3.5 | Silencing of SDCBP2-AS1 stabilized β-catenin and prohibited transcriptional activities

To identify the putative targets of SDCBP2-AS1, RNA-seq was performed to obtain the transcriptional profiles of BGC823 cells following knockdown of SDCBP2-AS1. Of 301 differentially expressed genes, 51 were upregulated and 250 were downregulated in the SDCBP2-AS1-knockdown group (Figure 5A). Furthermore, GSEA of the RNA-seq data indicated that knockdown of SDCBP2-AS1 was positively associated with overexpression of β-catenin (Figure 5B). The subcellular localization of lncRNAs is related to function [29]. SDCBP2-AS1 was mostly located in the cytoplasm and associated with β-catenin expression, suggesting that SDCBP2-AS1 interfered with the degradation of β-catenin [30]. For confirmation, Western blotting analysis showed that knockdown of SDCBP2-AS1 significantly increased the protein levels of β-catenin and hnRNP
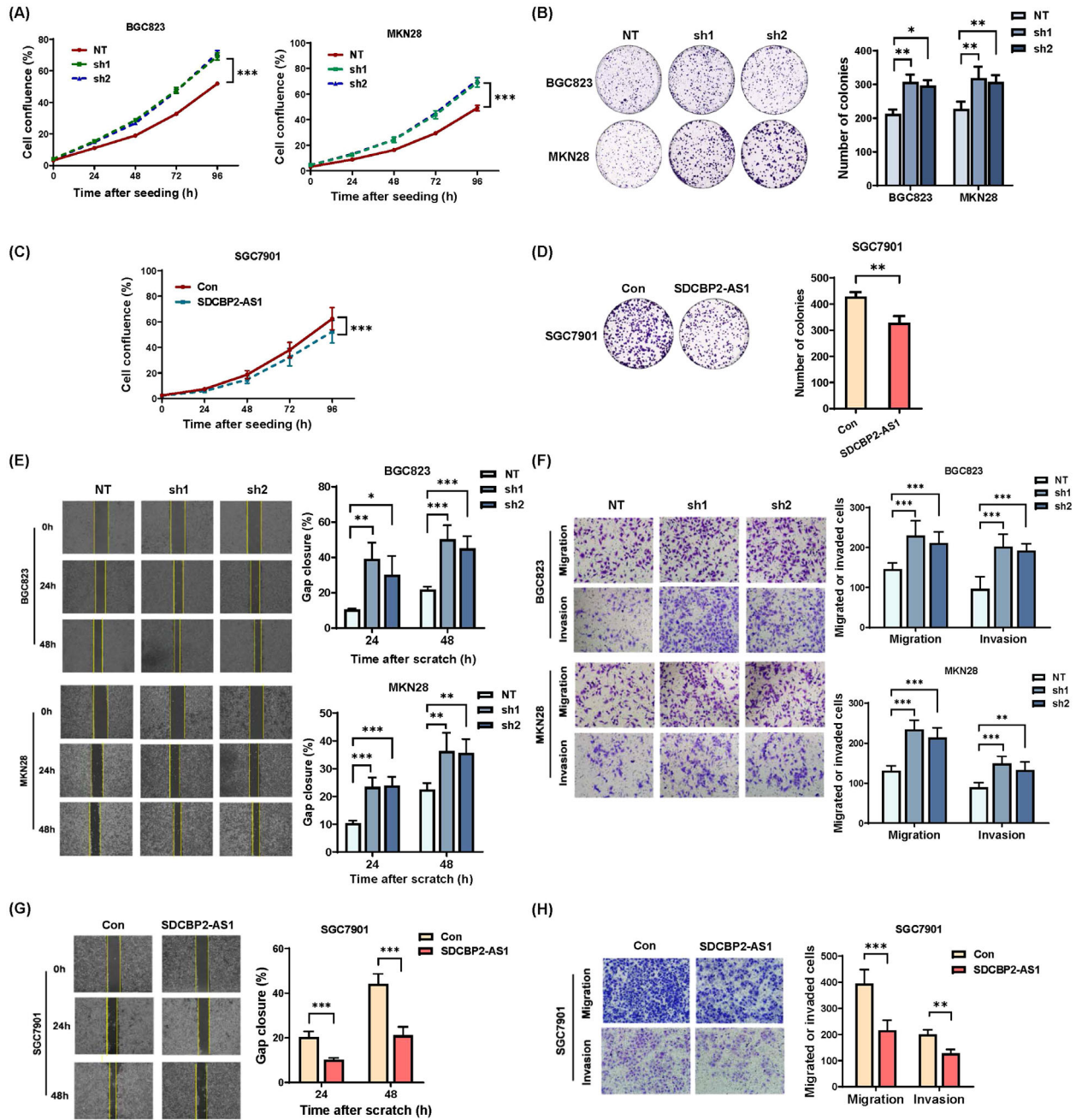
FIGURE 2 SDCBP2-AS1 suppressed GC cell proliferation and metastasis in vitro. (A-B) The proliferation and colony formation assay of stable SDCBP2-AS1-knockdown BGC823 and MKN28 cells. (C-D) The proliferation and colony formation assay of stable SDCBP2-AS1-overexpressing SGC7901 cells. (E-H) The results of wound healing and transwell assay of SDCBP2-AS1-knockdown BGC823 and MKN28 cells and SDCBP2-AS1-overexpressing SGC7901 cells, respectively. Data are presented as the mean ± SD. *$P < 0.05$, **$P < 0.01$, ***$P < 0.001$. Abbreviations: SDCBP2-AS1, syndecan binding protein 2 antisense RNA 1; GC, gastric cancer; NT, non-target; sh, small harpin RNA; Con, empty vector control; SD, standard deviation.

K in BGC823 and MKN28 cells, while SGC7901 cells overexpressing SDCBP2-AS1 had lower expression levels of β-catenin and hnRNP K (Figure 5C). Consistently, IHC staining showed that the expression of β-catenin was increased both in SDCBP2-AS1 low group of our patient cohort and in xenograft tumors formed by SDCBP2-AS1-knockdown BGC823 cells (Supplementary Figure S5A-C).

Additionally, Western blotting analysis showed that knockdown of SDCBP2-AS1 resulted in lower expression of β-catenin in the cytoplasm and higher expression in the nucleus (Figure 5D). Opposite results were obtained for hnRNP K. The results of the IF assay demonstrated that SDCBP2-AS1 altered the shuttling of β-catenin between the nucleus and cytoplasm in GC cells (Figure 5E). The
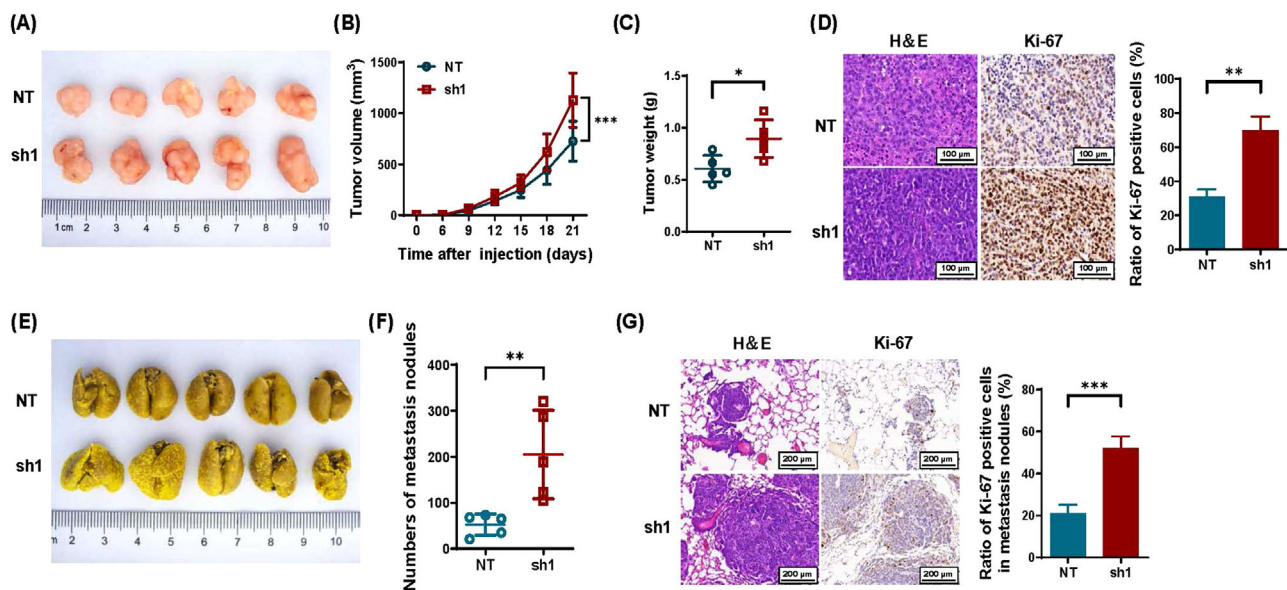
FIGURE 3 SDCBP2-AS1 suppressed growth and metastasis of GC cells in vivo. (A-D) Representative images (A) and xenograft quantification (B-D) of nude mice (5 mice/group) injected with stable SDCBP2-AS1-knockdown BGC823 cells (sh1) or with NT control cells. (B) Tumor volumes were calculated after injection every 3 days for 21 days. (C) Tumor weights are presented as the mean ± SD. (D) The tumor sections were subjected to staining with H&E and IHC analysis of Ki-67. (E) Representative images of metastatic sites in the lungs of nude mice injected via the tail vein with BGC823 cells stably transfected with the NT control or sh1 (5 mice/group). (F) Quantification of metastatic foci in lung tissues. (G) Representative images of H&E staining and IHC analysis of Ki-67 of metastatic sites in lung tissues. The intensity of Ki-67 staining was quantified. Data are presented as the mean ± SD. *$P < 0.05$, **$P < 0.01$, ***$P < 0.001$. Abbreviations: SDCBP2-AS1, syndecan binding protein 2 antisense RNA 1; GC, gastric cancer; NT, non-target; sh, small harpin RNA; H&E, hematoxylin and eosin; IHC, immunohistochemical; SD, standard deviation.

results of the TOP/FOP-flash luciferase assays showed that β-catenin signaling was activated in SDCBP2-AS1-knockdown cells (Figure 5F). In addition, the results of RT-qPCR and Western blotting analyses showed that stable overexpression or knockdown of SDCBP2-AS1 altered the expression patterns of genes downstream of β-catenin (i.e., *CCND1, MYC*, and *MMP7*). Translocation of β-catenin activated the Wnt signaling pathway, especially via Wnt3a, but not Wnt5a (Figure 5G-H). Also, the Akt and Erk signaling pathways were activated in SDCBP2-AS1-knockdown BGC823 cells, while the Erk pathway was repressed in SGC7901 cells overexpressing SDCBP2-AS1 (Supplementary Figure S5D-E). Taken together, these results demonstrate that the knockdown of SDCBP2-AS1 helped to stabilize β-catenin and activate the canonical Wnt signaling pathway.

3.6 | SDCBP2-AS1 destabilized β-catenin by blocking SUMOylation of hnRNP K in GC cells

Since SDCBP2-AS1 was found to regulate the protein levels of β-catenin and hnRNP K in different directions, SDCBP2-AS1 might also regulate post-transcriptional modifications.

Hence, the protein synthesis inhibitor CHX was used to evaluate the effect of SDCBP2-AS1 on the stability of β-catenin. After treatment with CHX, the protein synthesis of β-catenin decreased significantly in all groups, implying that knockdown of SDCBP2-AS1 or overexpression of SDCBP2-AS1 did not affect the protein synthesis of β-catenin (Figure 6A). In addition, after incubation with the proteasome inhibitor MG132, knockdown and overexpression of SDCBP2-AS1 had similar effects on the degradation of β-catenin in GC cells (Figure 6B). SDCBP2-AS1 regulated the degradation, but not synthesis, of β-catenin. IP analysis was performed to determine whether SDCBP2-AS1 is involved in forming a degradation complex targeting endogenous β-catenin. Since APC, Axin1, and GSK3β are the major components that induce the degradation of β-catenin, the interaction between β-catenin and the destruction complex decreased in the absence of SDCBP2-AS1 (Figure 6C), suggesting that SDCBP2-AS1 may interfere with degradation of β-catenin. Consistently, overexpression of SDCBP2-AS1 facilitated ubiquitination and degradation of β-catenin (Figure 6C) by binding to hnRNP K. In the absence of SDCBP2-AS1, ubiquitination of β-catenin was incomplete (Figure 6D). To further investigate the capacity of SDCBP2-AS1 to destabilize β-catenin and given that the RNA pull-down
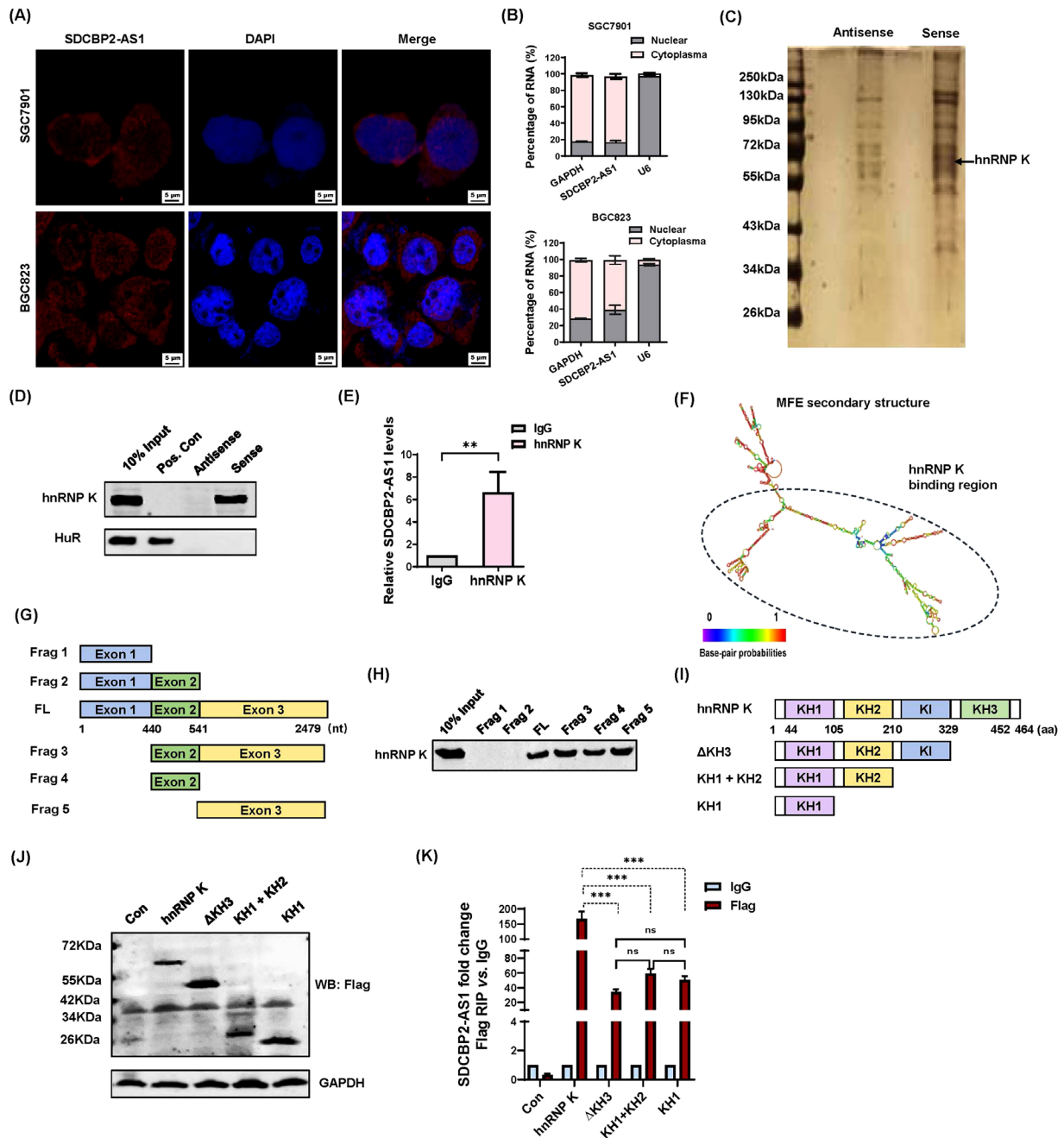
FIGURE 4 SDCBP2-AS1 interacted with hnRNP K in the cytoplasm. (A) RNA-FISH analysis of SDCBP2-AS1 in the cytoplasmic (red) and nuclear (blue) fractions of SGC7901 and BGC823 cells. (B) Nuclear-cytoplasmic RNA fractionation assays showed that SDCBP2-AS1 was mainly located in the cytoplasm of SGC7901 and BGC823 cells. (C) RNA pull-down analysis of biotinylated or antisense SDCBP2-AS1 to identify associated proteins. After silver staining, bands were excised and analyzed by mass spectrometry, which showed that hnRNP K interacts with SDCBP2-AS1 in BGC823 cells. (D) Western blotting analysis of proteins collected from the SDCBP2-AS1 pull-down assay using an antibody against hnRNP K in BGC823 cells. (E) RNA-IP analysis of BGC823 cells using antibodies against hnRNP K or IgG. The precipitated RNA was used for RT-qPCR analysis. Enrichment of SDCBP2-AS1, as determined by RIP analysis of hnRNP K, was relative to the IgG control, showing that SDCBP2-AS1 interacted with hnRNP K. (F) The predicted secondary structure of SDCBP2-AS1 RNA. (G) A schematic diagram of full-length SDCBP2-AS1 and truncated fragments. (H) In vitro transcribed biotinylated RNA of different constructs of SDCBP2-AS1 associated with hnRNP K were detected by Western blotting analysis. (I) RIP assays were performed using an anti-Flag antibody in BGC823 cells stably transfected with Flag-tagged hnRNP K or deletion mutants. (J) Western blotting analysis was conducted to evaluate the expression of Flag-tagged hnRNP K or deletion mutants. (K) RT-qPCR analysis was used to measure enrichment of SDCBP2-AS1. Data are presented as the mean ± SD. *P < 0.05, **P < 0.01, ***P < 0.001. Abbreviations: SDCBP2-AS1, syndecan binding protein 2 antisense RNA 1; GC, gastric cancer; FISH, fluorescence in situ hybridization; GAPDH, glyceraldehyde 3-phosphate dehydrogenase; U6, U6 small nuclear RNA; hnRNP K, heterogeneous nuclear ribonucleoprotein K; Frag, fragment; Pos. Con, positive control; Con, empty vector control; RIP, RNA immunoprecipitation; MFE, minimum free energy; RT-qPCR, quantitative real-time polymerase chain reaction; SD, standard deviation.
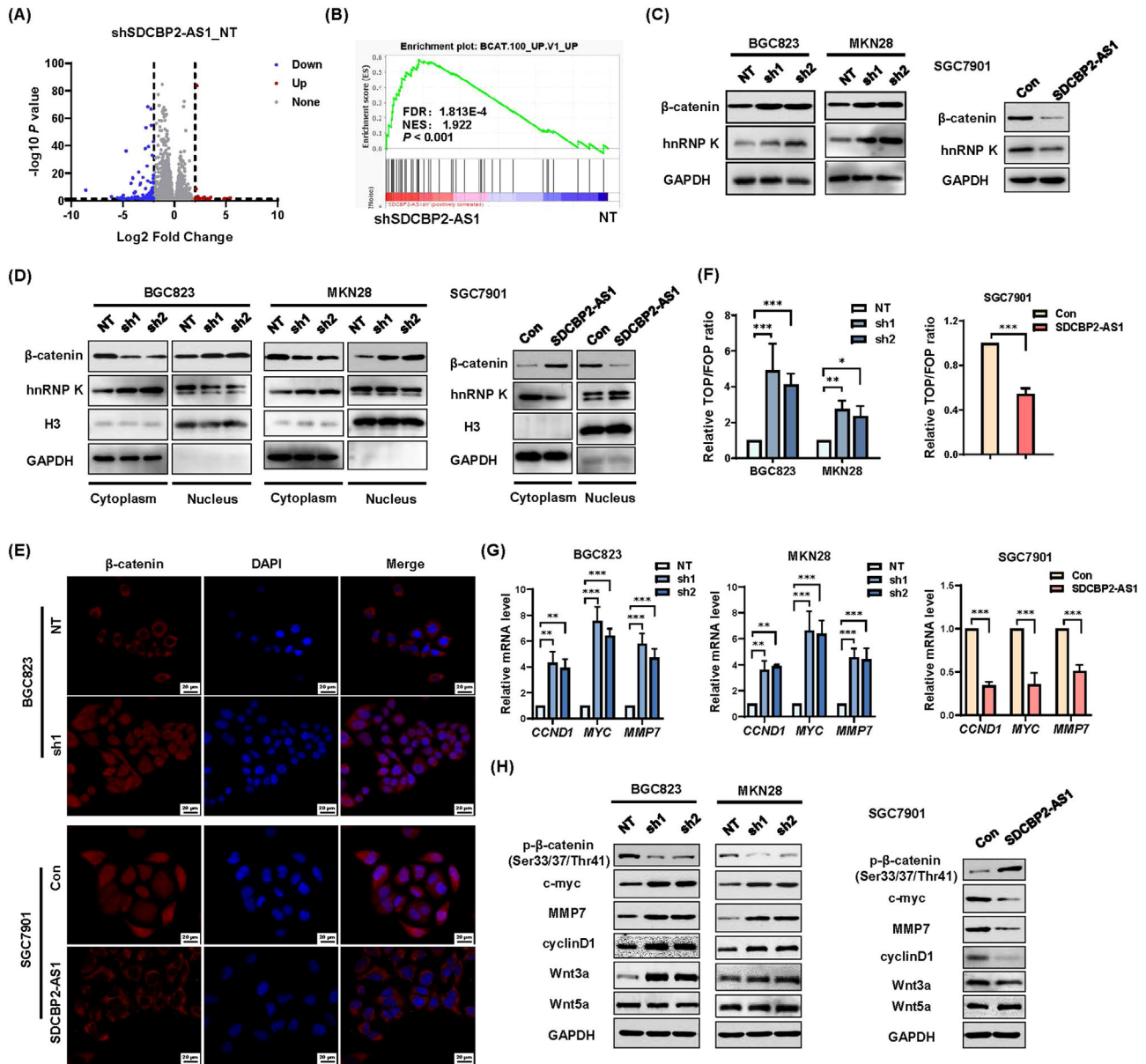
FIGURE 5 Silencing of SDCBP2-AS1 stabilized β-catenin and prohibited transcriptional activity. (A) Clustering volcano plot of differentially expressed genes in stable SDCBP2-AS1-knockdown BGC823 cells or its NT control. (B) Identification of enriched oncogenic signatures gene sets associated with SDCBP2-AS1 knockdown by GSEA. (C) β-catenin and hnRNP K protein levels in whole-cell lysates were analyzed by Western blotting analysis. (D) The nuclear and cytoplasmic protein levels of hnRNP K and β-catenin in BGC823 or MKN28 cells stably transfected with the NT control or sh1 or in SGC7901 cells stably overexpressing the empty vector control (Con) or SDCBP2-AS1 as determined by Western blotting analysis. GAPDH served as the cytosolic control, and histone H3 was used to validate the nuclear content. (E) IF confocal images revealing localization of β-catenin in SDCBP2-AS1-knockdown BGC823 cells and SDCBP2-AS1-overexpressing SGC97901 cells. (F) Results of the TOP/FOP-flash luciferase assays indicating the relative transcriptional activity of β-catenin in BGC823 or MKN28 cells stably transfected with the NT control or sh1 and in SGC7901 cells stably overexpressing SDCBP2-AS1. (G-H) mRNA expression levels of *MYC*, *CCND1*, and *MMP7* as detected by RT-qPCR analysis (G) and protein levels of c-Myc, cyclin D1, MMP7, p-β-catenin (Ser33/37/Thr41), Wnt3a, and Wnt5a as detected by Western blotting analysis (H) in BGC823 or MKN28 cells after knockdown of SDCBP2-AS1 and in SGC7901 cells overexpressing SDCBP2-AS1. GAPDH served as the endogenous control. **$P < 0.01$, ***$P < 0.001$. Abbreviations: SDCBP2-AS1, syndecan binding protein 2 antisense RNA 1; GC, gastric cancer; GSEA, gene set enrichment analysis; NT, non-target; sh, small harpin RNA; Con, empty vector control; FDR, false discovery rate; NES, enrichment score; IF, immunofluorescence; RT-qPCR, quantitative real-time polymerase chain reaction; hnRNP K, heterogeneous nuclear ribonucleoprotein K; H3, histone 3; GAPDH, glyceraldehyde 3-phosphate dehydrogenase; MMP7, matrix metallopeptidase 7; CCND1, cyclin D1; p-β-catenin, phospho-β-catenin.
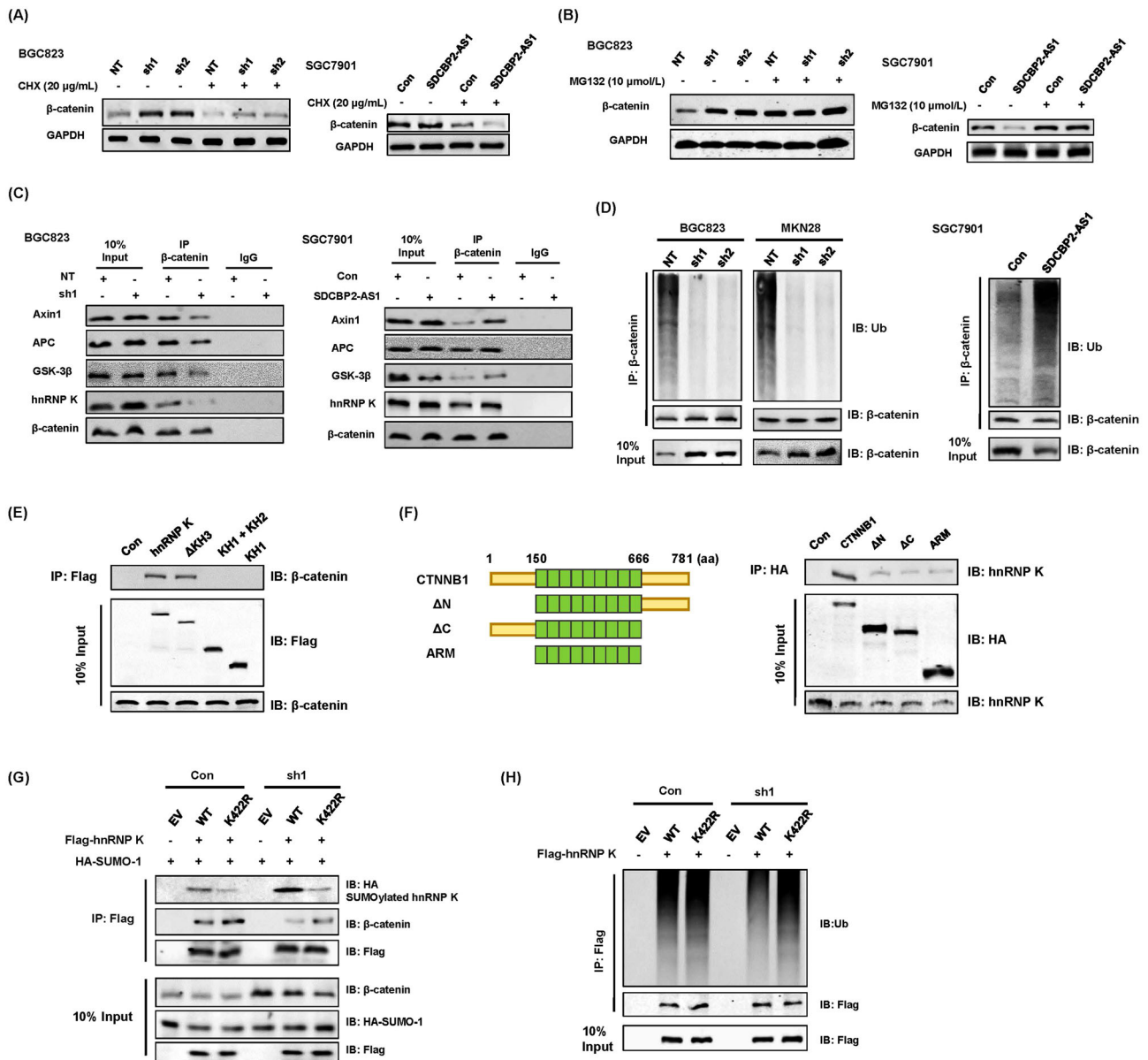
FIGURE 6 SDCBP2-AS1 destabilized β-catenin by blocking SUMOylation of hnRNP K. (A) Cells were treated with CHX (20 μg/mL) for 4 h before harvest. (B) Cells were treated with MG132 (10 μmol/L) for 8 h before harvest. The protein levels of β-catenin were measured in BGC823 cells after the knockdown of SDCBP2-AS1 or SGC7901 cells overexpressing SDCBP2-AS1 as determined by Western blotting analysis. (C) Extracts of BGC823 cells after knockdown of SDCBP2-AS1 or SGC7901 cells overexpressing SDCBP2-AS1 were used for IP analysis with antibodies against β-catenin or IgG as a control. Western blotting analysis of β-catenin, APC, Axin1, GSK3β, and hnRNP K. (D) SDCBP2-AS1 regulated ubiquitination of β-catenin. IP assays of endogenous β-catenin in cell lines with SDCBP2-AS1 knockdown or overexpression, followed by Western blotting analysis with antibodies against ubiquitin and β-catenin. (E-F) BGC823 cells were transfected with Flag-tagged hnRNP K truncation constructs (E) or HA-tagged β-catenin truncation constructs (F) to identify the interaction domains between hnRNP K and β-catenin. (G) SDCBP2-AS1 knockdown in BGC823 cells overexpressing HA-tagged SUMO-1 and Flag-tagged wild-type hnRNP K or the K422R mutant. Cell lysates were subjected to IP analysis followed by Western blotting analysis with antibodies against Flag, HA and β-catenin. (H) After the knockdown of SDCBP2-AS1, BGC823 cells overexpressed Flag-tagged wild-type hnRNP K or the K422R mutant. Cell lysates were subjected to IP and Western blotting analysis with antibodies against Flag and ubiquitin. Abbreviations: SDCBP2-AS1, syndecan binding protein 2 antisense RNA 1; CHX, cycloheximide; IP, immunoprecipitation; APC, adenomatous polyposis coli; GSK3β, glycogen synthase kinase 3 beta; hnRNP K, heterogeneous nuclear ribonucleoprotein K; HA, hemagglutinin; GAPDH, glyceraldehyde 3-phosphate dehydrogenase; Ub, ubiquitin; ARM, armadillo repeats; NT, non-target; sh, small harpin RNA; Con, empty vector control; EV, empty vector; WT, wildtype; SUMO-1, small ubiquitin like modifier 1.

assay showed that SDCBP2-AS1 did not directly interact with β-catenin or β transducin repeat-containing protein (β-TrCP) (Supplementary Figure S6A), the ability of SDCBP2-AS1 to regulate interactions between β-catenin and hnRNP K was investigated. Hence, a series of Flag-tagged truncated hnRNP K protein was constructed as described in the preceding text, and the protein domain mapping study indicated that the KH3 and KI domains of hnRNP K were essential for its interactions with β-catenin (Figure 6E). Meanwhile, immunnoprecipitation of HA-tagged β-catenin truncation mutants showed all domains of β-catenin were involved in its interactions with hnRNP K, although the full length had the greatest binding ability (Figure 6F). In addition, SDCBP2-AS1 mainly interacted with the KH3 domain of hnRNP K. Several post-translational modification sites have been reported in the KH3 region, such as the lysine residue at position 422, which was identified as the major SUMOylation site of hnRNP K [31, 32]. Hence, the ability of SDCBP2-AS1 to regulate post-translational modifications of hnRNP K was investigated, especially SUMOylation and ubiquitination of the KH3 domain. Flag-tagged wild-type hnRNP K and the K422R mutant showed that the mutant interfered with SUMOylation of hnRNP K (Supplementary Figure S6B). Knockdown of SDCBP2-AS1 increased SUMOylation of the wild-type, but not the K422R mutant (Figure 6G), and decreased endogenous poly-ubiquitination of hnRNP K (Figure 6H). As compared with the K422R mutant, SDCBP2-AS1 altered SUMOylation by blocking the specific active site of the KH3 domain in the spatial structure. These results indicate that knockdown of SDCBP2-AS1 led to accumulation of β-catenin in the cytoplasm and subsequent nuclear translocation via stabilization of β-catenin in GC cells.

3.7 | The tumor-suppressor functions of SDCBP2-AS1 were partially exerted through interplay with hnRNP K

SGC7901 cells with stable knockdown of hnRNP K were established to assess the interactions between SDCBP2-AS1 and hnRNP K in GC cells (Supplementary Figure S7A). In addition, SDCBP2-AS1 was overexpressed to determine whether hnRNP K is a key mediator. Silencing of hnRNP K eliminated the tumor suppressor functions of SDCBP2-AS1, including cell proliferation and migration (Figure 7A-C). The results of the IF and Western blotting assays showed that without hnRNP K, SDCBP2-AS1 failed to facilitate nuclear translocation of β-catenin in GC cells (Figure 7D-E). In addition, the results of the TOP/FOP-flash luciferase, qPCR, and Western blotting assays showed that without hnRNP K, SDCBP2-AS1 could not acti-

vate transcription of downstream target genes and the Wnt/β-catenin pathway (Figure 7F-H). In xenograft tumor models, stable knockdown of hnRNP K in SGC7901 cells erased the differences in growth rate and tumor weight caused by overexpression of SDCBP2-AS1 (Figure 7I-K). In the lung metastasis model, knockdown of hnRNP K also attenuated the impacts of SDCBP2-AS1 overexpression on the metastatic potential of GC cells (Supplementary Figure S7B-C). These results demonstrated that SDCBP2-AS1 inhibited tumorigenicity via hnRNP K as shown in Figure 8.

4 | DISCUSSION

Although many lncRNAs with altered expression have been reported in gastric tumorigenesis, the functional roles and molecular mechanisms of many GC-specific lncRNAs have not been determined. In this study, SDCBP2-AS1 was identified as a novel tumor suppressor in GC tumorigenesis and metastasis. Comparisons of the expression patterns of SDCBP2-AS1 in GC tissues and validation of the Gene Expression Omnibus data showed that low expression of SDCBP2-AS1 was associated with poor prognosis of GC patients. A series of in vitro and in vivo experiments showed that knockdown of SDCBP2-AS1 significantly promoted tumorigenesis and metastasis.

An analysis of public datasets showed that SDCBP2-AS1 was significantly associated with DFS in patients with thyroid cancer [33]. However, the biological functions of SDCBP2-AS1 were not investigated in that study. SDCBP2-AS1 was shown to regulate ependymin-related 1 (EPDR1) by competitively binding to miR-100-5p, which targets EPDR1, thereby inhibiting the progression of ovarian cancer [34]. Whether SDCBP2-AS1 also functions as a competing endogenous RNA in GC is worthy of future research. In the present study, we focused on identifying the protein partner and their post-transcriptional modifications pattern of SDCBP2-AS1.

The function of lncRNAs is largely determined by subcellular location [35, 36]. According to previous reports, lncRNAs located in the nucleus, such as Pvt1 oncogene (PVT-1) and homeobox A11 antisense RNA (HOXA11-AS), regulate transcription [37, 38], while those located in the cytoplasm, such as small nucleolar RNA host gene 5 (SNHG5) and urothelial cancer associated 1 (UCA1), act as sponges for microRNAs to regulate the expression of related mRNAs [39, 40] and others are involved in the regulation of cellular signaling pathways [41–43]. In the present study, RNA-FISH was conducted to determine the function of SDCBP2-AS1 and elucidate the molecular mechanisms in GC cells. Further, the RNA-seq results showed a significant connection between SDCBP2-AS1
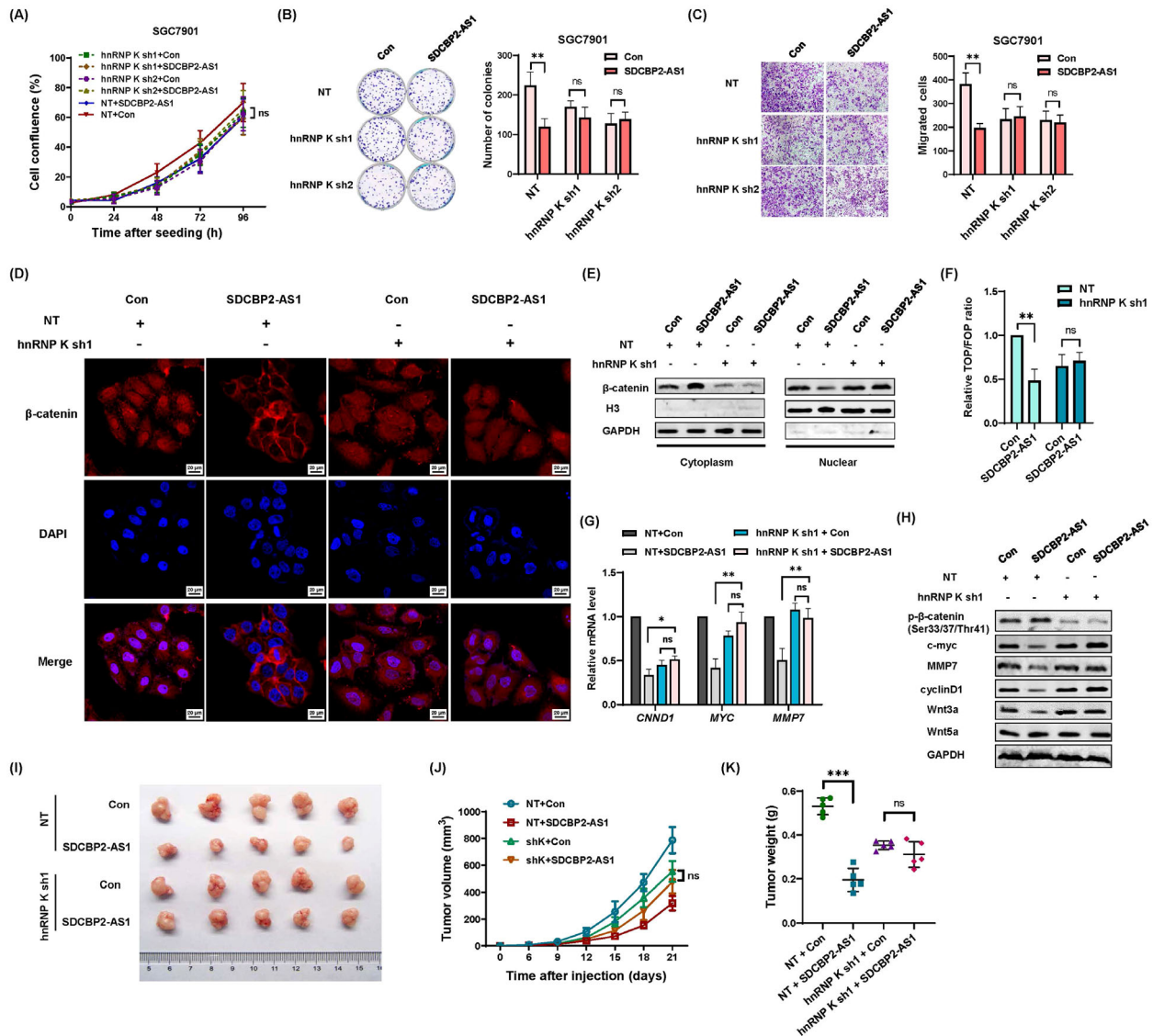
FIGURE 7 SDCBP2-AS1 exerted a tumor-suppressor function partially through interplay with hnRNP K. (A-C) The results of the cell proliferation (A), colony formation (B), and transwell assays (C) of SGC7901 cells stably transfected with the NT or sh-hnRNP K (sh1 and sh2) and sequtially transfected with the Con or SDCBP2-AS1. Knockdown of hnRNP K blocked SDCBP2-AS1's effects. (D-E) IF confocal images (D) and Western blotting analysis (E) of the nuclear and cytoplasmic protein levels of hnRNP K and β-catenin showed that knockdown of hnRNP K reversed the effects of SDCBP2-AS1 overexpression through localization of β-catenin in SGC7901 cells. (F) The results of the TOP/FOP-flash luciferase assays indicating changes in the relative transcriptional activity of β-catenin in SGC7901 cells after knockdown of hnRNP K or overexpression of SDCBP2-AS1. (G) RT-qPCR analysis of the mRNA levels (G) of *MYC*, *CCND1*, and *MMP7*. (H) Western blotting analysis of the protein levels (H) of c-Myc, cyclin D1, MMP7, p-β-catenin (Ser33/37/Thr41), Wnt3a, and Wnt5a. GAPDH served as the endogenous control. (I-K) Representative images (I), tumor volume growth curves (J), and tumor weight at the end points (K) of xenografts in athymic nude mice formed by subcutaneous injection of SGC7901 cells stably transfected with Con, SDCBP2-AS1, the NT control, or hnRNP K sh1 (5 mice/group). ***$P < 0.001$. Abbreviations: SDCBP2-AS1, syndecan binding protein 2 antisense RNA 1; NT, non-target; shK, known down hnRNP K with small harpin RNA; Con, empty vector control; IF, immunofluorescence; RT-qPCR, quantitative real-time polymerase chain reaction; hnRNP K, heterogeneous nuclear ribonucleoprotein K; H3, histone 3; GAPDH, glyceraldehyde 3-phosphate dehydrogenase; MMP7, matrix metallopeptidase 7; p-β-catenin, phospho-β-catenin.

and β-catenin, which was confirmed by the Western blotting and TOP/FOP-flash luciferase assay results. Knockdown of SDCBP2-AS1 stabilized β-catenin accumulation in the cytoplasm and its subsequent translocation into the nucleus, resulting in high expression of downstream

target genes [15]. Moreover, cytoplasmic localization of SDCBP2-AS1 promoted the degradation of β-catenin in GC cells. The lncRNA pancEts-1 was reported to interact with both hnRNP K and β-catenin to activate transcription [44], and solute carrier organic anion transporter family
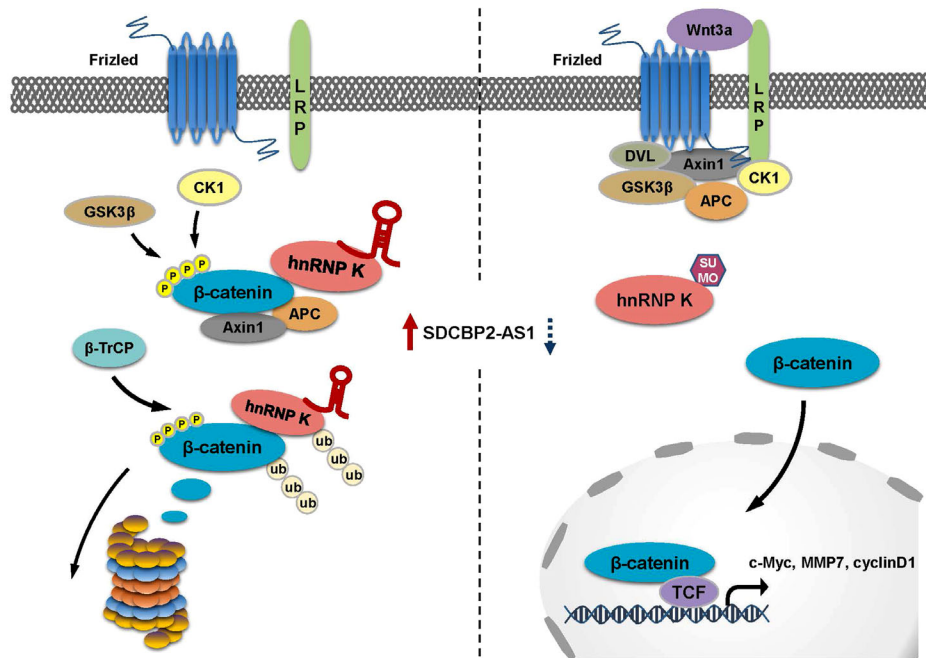
FIGURE 8 Schematic illustrating the mechanism of SDCBP2-AS1-induced suppression of tumorigenesis in GC. SDCBP2-AS1 regulates SUMOylation and ubiquitination of hnRNP K. SDCBP2-AS1 blocks the major SUMOylation site of hnRNP K, which increases ubiquitination of hnRNP K and β-catenin, and degradation of β-catenin. Knockout of SDCBP2-AS1 increases SUMOylation of hnRNP K and translocation of β-catenin to the nucleus for transcription. Abbreviations: SDCBP2-AS1, syndecan binding protein 2 antisense RNA 1; APC, adenomatous polyposis coli; β-TrCP, β-transducin repeat-containing protein; CK1, casein kinase1; Dvl, disheveled, dsh homolog; GSK3β, glycogen synthase kinase 3 beta; hnRNP K, heterogeneous nuclear ribonucleoprotein K; LRP, low-density lipoprotein receptor-related protein; TCF, T-cell factor enhancer-binding factor; SUMO, SUMOylation.

member 4A1 antisense RNA 1 (SLCO4A1-AS1) bound to β-catenin was found to block the interaction between β-catenin and GSK3β [45]. However, the results of the RNA pull-down assay showed that SDCBP2-AS1 directly bound to hnRNP K, but not β-catenin. The IP assay showed that when SDCBP2-AS1 was silenced, hnRNP K was still able to directly interact with endogenous β-catenin, but not as strongly as in the presence of SDCBP2-AS1. Therefore, SDCBP2-AS1 assisted in the interaction between hnRNP K and β-catenin, thereby effectively regulating the degradation of β-catenin and achieving the effect of suppressing tumorigenesis. The novel lncRNA human Fas-activated serine/threonine kinase (hFAST), located in the cytoplasm of human embryonic stem cells, maintained pluripotency of the cells by disrupting the interaction between β-TrCP and β-catenin, resulting in reduced degradation of β-catenin [46]. In the present study, the RNA pull-down assay did not detect direct interactions between SDCBP2-AS1 and β-TrCP, suggesting that SDCBP2-AS1 promoted degradation of β-catenin via hnRNP K in GC cells.

The results of the RNA pull-down and RIP assays of different truncated mutants of SDCBP2-AS1 and hnRNP K showed that the secondary structures of RNAs were important for binding to proteins. As previously reported, the KH domain was the major RNA/DNA-binding domain of hnRNP K [47, 48]. In the present study, the KH3 domain of hnRNP K was most readily bound to SDCBP2-AS1, although the other domains also bound to SDCBP2-AS1, indicating strong binding capacity between SDCBP2-AS1 and hnRNP K. Previous studies have reported that lncRNA-OG, lncRNA-p21, lncRNA THRIL, and LINC01354 physically associate with other members of the hnRNP family to mediate transcriptional regulation [26, 49-51]. The present study demonstrated that SDCBP2-AS1 bound to the KH3 domain and blocked the major SUMOylation site of hnRNP K, thereby regulating SUMOylation and ubiquitination of hnRNP K to further facilitate ubiquitination of β-catenin. Furthermore, SDCBP2-AS1 was found to promote phosphorylation of cytosolic β-catenin (Ser33/37/Thr41) as a part of the degradation step. Moreover, ubiquitinated hnRNP K might spatiotemporally recruit other E3 ubiquitin ligases, such as β-TrCP, a major regulator of β-catenin degradation.

Silencing of hnRNP K almost completely abolished the biological function of SDCBP2-AS1, suggesting that the function of SDCBP2-AS1 is mediated by hnRNP K. hnRNP K is shuttled between the cytoplasm and nucleus and interacts with both nucleic acids and proteins, thereby participating in many cellular functions, including transcription, translation, mRNA splicing, and chromatin

remodeling [52, 53]. Various post-translational modifications (i.e., phosphorylation, ubiquitination, SUMOylation, and methylation) determine the biological functions of hnRNP K [54, 55]. In the present study, knockdown of SDCBP2-AS1 increased the cytoplasmic fraction of hnRNP K and inhibited complex formation with β-catenin in the nucleus. This phenomenon of SDCBP2-AS1 in GC contradicts a previous report that hnRNP K and β-catenin were translocated to the nucleus simultaneously [44]. As a possible explanation for this discrepancy, SUMOylation and ubiquitination serve to rapidly change the activity and abundance of hnRNP K in response to different stress conditions in the cytoplasm [56]. Alternatively, β-catenin-induced massive abundance of pre-RNA requires the accumulation of hnRNP K in the cytoplasm to manage RNA processing.

Although the results of this study revealed that SDCBP2-AS1 could interact with hnRNP K and assist in the degradation of β-catenin, the precise site of hnRNP K binds to SDCBP2-AS1 remains unclear. A docking model of SDCBP2-AS1 and hnRNP K are needed in our future study, which will spatially demonstrate how the ubiquitinated β-catenin/hnRNP K complex regulates phosphorylation of β-catenin and other unknown proteins involved in the degradation process.

5 | CONCLUSIONS

In summary, we reported SDCBP2-AS1 as a novel tumor suppressor lncRNA that inhibited proliferation and metastasis of GC cells. The tumor suppressor function of SDCBP2-AS1 via directly binding to hnRNP K regulated post-transcriptional modifications of hnRNP K and β-catenin, thereby promoting degradation of β-catenin. Consistently, stabilization of β-catenin via loss of SDCBP2-AS1 resulted in poor prognosis of GC patients, demonstrating that SDCBP2-AS1 may be a potential diagnostic and prognostic biomarker for GC patients.

AUTHOR CONTRIBUTIONS
Conceived the hypothesis, Jing Han and Menglin Nie; Performed the experiments, Jing Han, Menglin Nie and Cong Chen; Designed and interpreted the results, Jing Han, Menglin Nie, Cong Chen, Xiaojing Cheng, Ting Guo, Xiaomei Li, Longtao Huangfu, and Hong Du; Wrote the manuscript, Jing Han, Menglin Nie and Cong Chen; Supervised the study, Xiaofang Xing and Jiafu Ji. All authors read and approved the final version of the manuscript.

CONFLICTS OF INTEREST
The authors declare no potential conflicts of interest.

DATA AVAILABILITY STATEMENT
Original RNA-sequencing data are available in the NCBI BioProject database (https://www.ncbi.nlm.nih.gov/bioproject/; BioProject ID: PRJNA832819). The datasets generated and/or analyzed during the current study are available from the corresponding author upon reasonable request.

ETHICS APPROVAL AND CONSENT TO PARTICIPATE
Informed consent was obtained from all patients. The study protocol was approved by the Ethics Committee of Peking University Cancer Hospital (approval no. 2018KT07).

CONSENT FOR PUBLICATION
Not applicable.

ORCID
Jing Han 🄳 https://orcid.org/0000-0001-6490-2052
Ting Guo 🄳 https://orcid.org/0000-0003-0199-5639

REFERENCES
1. Sung H, Ferlay J, Siegel RL, Laversanne M, Soerjomataram I, Jemal A, et al. Global Cancer Statistics 2020: GLOBOCAN Estimates of Incidence and Mortality Worldwide for 36 Cancers in 185 Countries. CA Cancer J Clin. 2021;71(3):209-49.
2. Xia C, Dong X, Li H, Cao M, Sun D, He S, et al. Cancer statistics in China and United States, 2022: profiles, trends, and determinants. Chin Med J (Engl). 2022;135(5):584-90.
3. Wang FH, Zhang XT, Li YF, Tang L, Qu XJ, Ying JE, et al. The Chinese Society of Clinical Oncology (CSCO): Clinical guidelines for the diagnosis and treatment of gastric cancer, 2021. Cancer Commun (Lond). 2021;41(8):747-95.

4. Chen W, Zheng R, Baade PD, Zhang S, Zeng H, Bray F, et al. Cancer statistics in China, 2015. CA Cancer J Clin. 2016;66(2):115-32.

5. Yang L, Ying X, Liu S, Lyu G, Xu Z, Zhang X, et al. Gastric cancer: Epidemiology, risk factors and prevention strategies. Chin J Cancer Res. 2020;32(6):695-704.

6. Djebali S, Davis CA, Merkel A, Dobin A, Lassmann T, Mortazavi A, et al. Landscape of transcription in human cells. Nature. 2012;489(7414):101-8.

7. Mercer TR, Dinger ME, Mattick JS. Long non-coding RNAs: insights into functions. Nat Rev Genet. 2009;10(3):155-9.

8. Ulitsky I, Bartel DP. lincRNAs: genomics, evolution, and mechanisms. Cell. 2013;154(1):26-46.

9. Batista PJ, Chang HY. Long noncoding RNAs: cellular address codes in development and disease. Cell. 2013;152(6):1298-307.

10. Tan P, Yeoh KG. Genetics and Molecular Pathogenesis of Gastric Adenocarcinoma. Gastroenterology. 2015;149(5):1153-62 e3.

11. Sun TT, He J, Liang Q, Ren LL, Yan TT, Yu TC, et al. LncRNA GClnc1 Promotes Gastric Carcinogenesis and May Act as a Modular Scaffold of WDR5 and KAT2A Complexes to Specify the Histone Modification Pattern. Cancer Discov. 2016;6(7):784-801.

12. Ooi CH, Ivanova T, Wu J, Lee M, Tan IB, Tao J, et al. Oncogenic pathway combinations predict clinical prognosis in gastric cancer. PLoS Genet. 2009;5(10):e1000676.

13. Cristescu R, Lee J, Nebozhyn M, Kim KM, Ting JC, Wong SS, et al. Molecular analysis of gastric cancer identifies subtypes associated with distinct clinical outcomes. Nat Med. 2015;21(5):449-56.

14. Clevers H. Wnt/beta-catenin signaling in development and disease. Cell. 2006;127(3):469-80.

15. Clevers H, Nusse R. Wnt/beta-catenin signaling and disease. Cell. 2012;149(6):1192-205.

16. Liu C, Li Y, Semenov M, Han C, Baeg GH, Tan Y, et al. Control of beta-catenin phosphorylation/degradation by a dual-kinase mechanism. Cell. 2002;108(6):837-47.

17. Huang HC, Wen XZ, Xue H, Chen RS, Ji JF, Xu L. Phosphoglucose isomerase gene expression as a prognostic biomarker of gastric cancer. Chin J Cancer Res. 2019;31(5):771-84.

18. Kong L, Zhang Y, Ye ZQ, Liu XQ, Zhao SQ, Wei L, et al. CPC: assess the protein-coding potential of transcripts using sequence features and support vector machine. Nucleic Acids Res. 2007;35(Web Server issue):W345-9.

19. Kang YJ, Yang DC, Kong L, Hou M, Meng YQ, Wei L, et al. CPC2: a fast and accurate coding potential calculator based on sequence intrinsic features. Nucleic Acids Res. 2017;45(W1):W12-W6.

20. Wang J, Ding Y, Wu Y, Wang X. Identification of the complex regulatory relationships related to gastric cancer from lncRNA-miRNA-mRNA network. J Cell Biochem. 2020;121(1):876-87.

21. Lin MF, Jungreis I, Kellis M. PhyloCSF: a comparative genomics method to distinguish protein coding and non-coding regions. Bioinformatics. 2011;27(13):i275-82.

22. Szasz AM, Lanczky A, Nagy A, Forster S, Hark K, Green JE, et al. Cross-validation of survival associated biomarkers in gastric cancer using transcriptomic data of 1,065 patients. Oncotarget. 2016;7(31):49322-33.

23. Wang X, Liang Q, Zhang L, Gou H, Li Z, Chen H, et al. C8orf76 Promotes Gastric Tumorigenicity and Metastasis by Directly Inducing lncRNA DUSP5P1 and Associates with Patient Outcomes. Clin Cancer Res. 2019;25(10):3128-40.

24. Nie ML, Han J, Huang HC, Guo T, Huangfu LT, Cheng XJ, et al. The novel lncRNA p4516 acts as a prognostic biomarker promoting gastric cancer cell proliferation and metastasis. Cancer Manag Res. 2019;11:5375-91.

25. Gurney A, Axelrod F, Bond CJ, Cain J, Chartier C, Donigan L, et al. Wnt pathway inhibition via the targeting of Frizzled receptors results in decreased growth and tumorigenicity of human tumors. Proc Natl Acad Sci U S A. 2012;109(29):11717-22.

26. Guo T, Wen XZ, Li ZY, Han HB, Zhang CG, Bai YH, et al. ISL1 predicts poor outcomes for patients with gastric cancer and drives tumor progression through binding to the ZEB1 promoter together with SETD7. Cell Death Dis. 2019;10(2):33.

27. Budczies J, Klauschen F, Sinn BV, Gyorffy B, Schmitt WD, Darb-Esfahani S, et al. Cutoff Finder: a comprehensive and straightforward Web application enabling rapid biomarker cutoff optimization. PLoS One. 2012;7(12):e51862.

28. Blasius M, Bartek J. ATM targets hnRNPK to control p53. Cell Cycle. 2013;12(8):1162-3.

29. Carlevaro-Fita J, Johnson R. Global Positioning System: Understanding Long Noncoding RNAs through Subcellular Localization. Mol Cell. 2019;73(5):869-83.

30. Yang G, Biswasa C, Lin QS, La P, Namba F, Zhuang T, et al. Heme oxygenase-1 regulates postnatal lung repair after hyperoxia: role of beta-catenin/hnRNPK signaling. Redox Biol. 2013;1:234-43.

31. Tsai HY, Fu SL, Tseng LM, Chiu JH, Lin CH. hnRNPK S379 phosphorylation participates in migration regulation of triple negative MDA-MB-231 cells. Sci Rep. 2019;9(1):7611.

32. Pelisch F, Pozzi B, Risso G, Munoz MJ, Srebrow A. DNA damage-induced heterogeneous nuclear ribonucleoprotein K sumoylation regulates p53 transcriptional activation. J Biol Chem. 2012;287(36):30789-99.

33. Rao Y, Liu H, Yan X, Wang J. In Silico Analysis Identifies Differently Expressed lncRNAs as Novel Biomarkers for the Prognosis of Thyroid Cancer. Comput Math Methods Med. 2020;2020:3651051.

34. Liu X, Liu C, Zhang A, Wang Q, Ge J, Li Q, et al. Long non-coding RNA SDCBP2-AS1 delays the progression of ovarian cancer via microRNA-100-5p-targeted EPDR1. World J Surg Oncol. 2021;19(1):199.

35. Chen LL. Linking Long Noncoding RNA Localization and Function. Trends Biochem Sci. 2016;41(9):761-72.

36. Ulitsky I. Evolution to the rescue: using comparative genomics to understand long non-coding RNAs. Nat Rev Genet. 2016;17(10):601-14.

37. Xu MD, Wang Y, Weng W, Wei P, Qi P, Zhang Q, et al. A Positive Feedback Loop of lncRNA-PVT1 and FOXM1 Facilitates Gastric Cancer Growth and Invasion. Clin Cancer Res. 2017;23(8):2071-80.

38. Sun M, Nie F, Wang Y, Zhang Z, Hou J, He D, et al. LncRNA HOXA11-AS Promotes Proliferation and Invasion of Gastric Cancer by Scaffolding the Chromatin Modification Factors PRC2, LSD1, and DNMT1. Cancer Res. 2016;76(21):6299-310.

39. Zhao L, Han T, Li Y, Sun J, Zhang S, Liu Y, et al. The lncRNA SNHG5/miR-32 axis regulates gastric cancer cell proliferation and migration by targeting KLF4. FASEB J. 2017;31(3):893-903.

40. Gong P, Qiao F, Wu H, Cui H, Li Y, Zheng Y, et al. LncRNA UCA1 promotes tumor metastasis by inducing miR-203/ZEB2 axis in gastric cancer. Cell Death Dis. 2018;9(12):1158.

41. Zhang H, Huang H, Xu X, Wang H, Wang J, Yao Z, et al. LncRNA HCG11 promotes proliferation and migration in gastric cancer via targeting miR-1276/CTNNB1 and activating Wnt signaling pathway. Cancer Cell Int. 2019;19:350.

42. Chen JF, Wu P, Xia R, Yang J, Huo XY, Gu DY, et al. STAT3-induced lncRNA HAGLROS overexpression contributes to the malignant progression of gastric cancer cells via mTOR signal-mediated inhibition of autophagy. Mol Cancer. 2018; 17(1):6.

43. Zhu K, Ren Q, Zhao Y. lncRNA MALAT1 overexpression promotes proliferation, migration and invasion of gastric cancer by activating the PI3K/AKT pathway. Oncol Lett. 2019;17(6):5335-42.

44. Li D, Wang X, Mei H, Fang E, Ye L, Song H, et al. Long Noncoding RNA pancEts-1 Promotes Neuroblastoma Progression through hnRNPK-Mediated beta-Catenin Stabilization. Cancer Res. 2018;78(5):1169-83.

45. Yu J, Han Z, Sun Z, Wang Y, Zheng M, Song C. LncRNA SLCO4A1-AS1 facilitates growth and metastasis of colorectal cancer through beta-catenin-dependent Wnt pathway. J Exp Clin Cancer Res. 2018;37(1):222.

46. Guo CJ, Ma XK, Xing YH, Zheng CC, Xu YF, Shan L, et al. Distinct Processing of lncRNAs Contributes to Non-conserved Functions in Stem Cells. Cell. 2020;181(3):621-36 e22.

47. Messias AC, Harnisch C, Ostareck-Lederer A, Sattler M, Ostareck DH. The DICE-binding activity of KH domain 3 of hnRNP K is affected by c-Src-mediated tyrosine phosphorylation. J Mol Biol. 2006;361(3):470-81.

48. Adolph D, Flach N, Mueller K, Ostareck DH, Ostareck-Lederer A. Deciphering the cross talk between hnRNP K and c-Src: the c-Src activation domain in hnRNP K is distinct from a second interaction site. Mol Cell Biol. 2007;27(5):1758-70.

49. Tang S, Xie Z, Wang P, Li J, Wang S, Liu W, et al. LncRNA-OG Promotes the Osteogenic Differentiation of Bone Marrow-Derived Mesenchymal Stem Cells Under the Regulation of hnRNPK. Stem Cells. 2019;37(2):270-83.

50. Bao X, Wu H, Zhu X, Guo X, Hutchins AP, Luo Z, et al. The p53-induced lincRNA-p21 derails somatic cell reprogramming by sustaining H3K9me3 and CpG methylation at pluripotency gene promoters. Cell Res. 2015;25(1):80-92.

51. Li Z, Chao TC, Chang KY, Lin N, Patil VS, Shimizu C, et al. The long noncoding RNA THRIL regulates TNFalpha expression through its interaction with hnRNPL. Proc Natl Acad Sci U S A. 2014;111(3):1002-7.

52. Barboro P, Ferrari N, Balbi C. Emerging roles of heterogeneous nuclear ribonucleoprotein K (hnRNP K) in cancer progression. Cancer Lett. 2014;352(2):152-9.

53. Xu Y, Wu W, Han Q, Wang Y, Li C, Zhang P, et al. New Insights into the Interplay between Non-Coding RNAs and RNA-Binding Protein HnRNPK in Regulating Cellular Functions. Cells. 2019;8(1).

54. Xu Y, Wu W, Han Q, Wang Y, Li C, Zhang P, et al. Post-translational modification control of RNA-binding protein hnRNPK function. Open Biol. 2019;9(3):180239.

55. Qin G, Tu X, Li H, Cao P, Chen X, Song J, et al. Long Noncoding RNA p53-Stabilizing and Activating RNA Promotes p53 Signaling by Inhibiting Heterogeneous Nuclear Ribonucleoprotein K deSUMOylation and Suppresses Hepatocellular Carcinoma. Hepatology. 2020;71(1):112-29.

56. Lee SW, Lee MH, Park JH, Kang SH, Yoo HM, Ka SH, et al. SUMOylation of hnRNP-K is required for p53-mediated cell-cycle arrest in response to DNA damage. EMBO J. 2012;31(23):4441-52.

SUPPORTING INFORMATION

Additional supporting information can be found online in the Supporting Information section at the end of this article.

How to cite this article: Han J, Nie M, Chen C, Cheng X, Guo T, Huangfu L, et al. SDCBP-AS1 destabilizes β-catenin by regulating ubiquitination and SUMOylation of hnRNP K to suppress gastric tumorigenicity and metastasis. Cancer Communications. 2022;42:1141–1161. https://doi.org/10.1002/cac2.12367